Atmos. Chem. Phys. Discuss.,
https://doi.org/10.5194/acp-2019-1013-AC1, 2020

Atmospheric Chemistry and Physics Discussions

Interactive comment on "Roll vortices induce new particle formation bursts in the planetary boundary layer" *by* Janne Lampilahti et al.

Janne Lampilahti et al.

janne.lampilahti@helsinki.fi

Received and published: 30 May 2020

We thank the referee for the constructive comments on our manuscript, please find our responses below.

Major comments

1. Measurement average : All measurements are performed at different frequency and the authors choose to average all the data over different periods (4 min, 12 min, 30min). They did not justify why they choose these periods. Why not using the same periods for all instruments ? The DMPS SD are not averaged what was the frequency for this instrument?

Answer: The time resolutions used were those of the processed data, we did not re-

Printer-friendly version

Discussion paper

average the processed data afterwards. We changed the text to better reflect this. The DMPS processed data had time resolution of 10 min, we also added this information to the text.

“The NAIS measured the particle number-size distribution in the mobility diameter range 2-42 nm and ion number-size distribution in the mobility diameter range 0.8-42 nm at 4 min time resolution. We used data from the positive polarity of the instrument.”

“The time resolutions of the DMPS and the NAIS were 10 min and 4 min respectively, from the NAIS we again used particle data from the positive polarity. The PSM measured particle number-size distribution between 1-2 nm and the time resolution was 12 min.”

2. Measurement location : Could you please justify that inlet height differences are unnoticeable on aerosol measurements ? Especially, when you used the synergy between anemometer at 125m above the ground with a CPC at 23m.

Answer: The vertical particle flux was calculated from a CPC and a 3d anemometer positioned at 23 m above ground. The anemometer at 125 m above ground was only used in wind data analysis. We removed the mention of the 125 m anemometer from the text since the results of this analysis are not shown in the text.

3. In general the figure labels are really long because you explained most of the time the way you used to process the data. I found it odd, especially because you are limited in word numbers. For example, I have many questions about Figure 9. From what I understood, figure 9 shows size distribution and formation rate calculations based on observations of geometric mean diameter.

Answer: We made the captions in Figures 2-9 shorter by moving some of the interpretation of the figure to the main text instead of keeping it in the caption. Figure 8 caption we kept the same since it describes a supporting case study and explaining it in detail in the main text would break the flow where it is mentioned as part of the GR

estimation.

- First of all, geometric mean diameter given in table 3 is observed at the end of the event, an hour after the beginning ? This is not clearly stated when the Dp values refer to.

Answer: At the measurement station the roll vortex induced new particle formation (RI-NPF) is observed as an intermittent, concentrated mode of sub-20 nm particles, with sudden beginning and end. One might describe it as a particle stripe in the sub-20 nm sizes. To obtain the geometric mean diameter for each RI-NPF reported in Table 3 we fitted a log-normal curve to the particle number-size distributions present in the RI-NPF and chose the peak value at the beginning of the RI-NPF observation as the geometric mean diameter that we report in Table 3.

In Table 3 caption we added that the geometric mean diameter is reported at the beginning of the RI-NPF:

“Dp = geometric mean particle diameter of roll-induced NPF event, determined at the beginning of the roll induced NPF observation”

- Then you use a constant GR of 1.9nm/h. Why ? You have measured the GR for each case. Then why using this value corresponding to GR from days that showed multiple subsequent roll-induced NPF events ? According to Table 3, the GR ranges from 0.8 to 4.3 nm/h. The use of GR value 2 times lower or larger might causes a lot of difference in the diameter growth and the formation rate.

- Moreover, I don’t understand the last sentence : Âń We then used random sampling (1000 samples), also varying the GR, to estimate 25th, 50th and 75th percentile values for the formation rates of 3- and 10-nm-sized particles ÂÅij . From this sentence, one can understand that the GR is not fixed anymore. What are the values used then ??? Also, you used 1000 random samples from what you calculated. Do you have 1000 samples from what you calculated ? You have 3 (GR variations ?) * One SD/hour *nb

of events (46) or did I miss something ?

- How do you control this random factor ? Could the 1000 samples belongs to one or 2 specific events ? If the GR is two times larger, what will be the error on the formation rate.

- And so you did all that to get formation rates that you measured directly ???

Answer: In order to clearly observe particle growth we had to see more than one RI-NPF event go over the station. We estimated the GR from the change in the geometric mean diameters in the subsequent RI-NPF events. This happened on 13/29 days in Table 3. In addition on 8 May 2013 the zeppelin flew through the same RI-NPF multiple times throughout the day for several hours, which also allowed us to observe the particle growth and calculate GR.

We changed the text to read:

"Multiple roll-induced NPF events during a single day were observed on 13/29 days. In these cases by looking at the change in particle diameter between subsequent roll-induced NPF events we were able to estimate the GR. In addition, on May 8, 2013 we could calculate the GR from a single roll-induced NPF event by following it with the zeppelin aircraft (Figure 8)."

From the 14 GR values we calculated the median, 25th and 75th percentile GRs. These represent the average GR for the RI-NPF particles in Table 3. We assumed that the underlying distribution of the GRs is a normal distribution with mean equal to the median GR and the standard deviation equal to the inter quartile range (IQR) of the GRs. From this normal distribution we then randomly sampled a GR.

Assuming that in Table 3 the particles in each RI-NPF case were formed at time t = 0 hours and that the GR remained constant, we estimated the time dt since the RI-NPF particles in Table 3 were formed using dt = Dp/GR, where Dp is the geometric mean diameter of the particles at the beginning of the RI-NPF observation.

This way we were able to put all the RI-NPF observations in Table 3 on a common time axis where the time is the time since particle formation. We then divided this time axis into 1-hour bins and in each bin calculated the median, 25th and 75th percentile particle number-size distribution. Again we assumed that the particle number-size distributions in each bin were normally distributed with mean equal to the median and standard deviation equal to the IQR. Then we randomly sampled a distribution from each bin and used the randomly sampled values to calculate the formation rate time series for 3 nm and 10 nm particles.

The particle size distribution displayed in Figure 9 consists of medians in each bin and the median GR was used to calculate the time since start of NPF.

We repeated the above random sampling 1000 times in order to obtain 1000 formation rate time series. From these formation rates we calculated the median, 25th and 75th percentile values. These are then our estimates for the average J3 and J10 plus their uncertainties, which are displayed in Figure 9.

In principle we could calculate formation rate for some individual cases. This means the case needs to have at least two subsequent RI-NPF events during the same day in order to estimate the GR, and also there needs to be particles for long enough time in the interesting size-range. Being this specific discards most of the data and we are left with just a couple of case studies. Instead we wanted to use a method that uses all the available observations. This allows us to get a formation rate that better represents the average and allows us to estimate the uncertainty.

We added a more explicit description to the text regarding the above procedure.

“We aggregated all the roll-induced NPF observations in Table 3 into 1-hour-averaged bins using the median GR and the geometric mean diameters of the particles, assuming that the particles were formed at t=0 hours (Figure 9).

Then we calculated the formation rates and their uncertainties. We assumed that the

roll-induced NPF GRs were normally distributed with mean equal to the median GR and standard deviation given by the magnitude of the IQR. Given the sampled GR we distributed the roll-induced NPF observations into 1-hour bins. For each 1-hour bin we assumed that the number-size distributions again followed a normal distribution with mean equal to the median and standard deviation given by the IQR. We randomly sampled a number-size distribution from each bin and calculated the formation rates based on that. We repeated this procedure 1000 times in order to estimate the J3 and J10 and their uncertainties shown in Figure 9."

4. Fraction of area : So you use a ratio of two periods and that give you a fraction area covered by the roll-induced NPF. Could you please explain the idea behind it ? I guess that this is related to the wind speed of the air mass over the site vs over the region. So, assuming both wind speeds are similar this is just a ratio of the horizontal extend of the NPF event when passing over the site and the horizontal extend of the NPF observed by the airborne instruments. What is the time shift between the aboard and grounded measurements ? Is the wind speed really constant during the whole period ?

Answer: First we assume that the RI-NPF extends a long distance along the length of the rolls, which is supported by the aircraft data. So then to estimate the area fraction we want to know what the spacing of RI-NPF is perpendicular to the rolls.

We needed more than one RI-NPF observation at the station during the same day in order to estimate this. Figure 1 shows how the rolls and by extension the RI-NPF move over the station if there is a difference in the direction of the roll axis and the mean wind direction.

If the wind conditions stay the same during the period when the multiple RI-NPF events move over the measurement station, then we can assume that the rolls move over the site at a steady pace. This means that the spatial extent across the RI-NPF events is directly proportional to the time interval we observe the RI-NPF events at the field station. This means that the time that subsequent RI-NPF events spent on top of the

measurement station divided by the total time it took for these RI-NPF events to move over the station is equal to the fraction of area covered by the RI-NPF events.

We can check the wind measurements from the mast at 33.6 m height above ground and see how constant they are (the 125 m measurement was not available for the whole time). For this we prepared Figure 2. Of course this does not tell us how the wind behaves in the rest of the boundary layer.

On most of the days the wind conditions do not fluctuate significantly during the multiple RI-NPF observations. On 2007-06-10 and 2017-04-24 the wind direction changes more than 100 degrees, and this could introduce some uncertainty, but would not have much effect on the final result.

The above analysis only requires ground-based observations. Since the flights covered a relatively small area we found them to be inadequate at estimating the spatial extent of RI-NPF in the direction perpendicular to rolls. One might argue that along the flight tracks in Figure 5 the concentrated particle areas took roughly half of the area on the track, which is in line with our findings from the above analysis.

We changed the text to better explain the method:

“In addition, we estimated the fraction of area covered by the roll-induced NPF. We assumed that the roll-induced NPF events extend much longer along the rolls, which is supported by the aircraft data. This means that for the area fraction we need to estimate what the spacing of the roll-induced NPF events is perpendicular to the direction of the rolls.

If the wind conditions stay the same during the period when the multiple RI-NPF events move over the station, then we can assume that the rolls move over the station at a steady pace. This means that dividing the time that subsequent roll-induced NPF events observed during the same day spent on top of the measurement station by the total time it took for the roll-induced NPF events to move over the site can be used as

an area fraction estimate. According to measurements from the mast, on average the wind conditions during the observations did not change significantly."

Minor remarks L161 – 171 : You could probably use figure 10 to ease the understanding. It would be useful !

Answer: We prepared Figure 1 to illustrate how rolls move over the measurement station perpendicular to the mean wind direction and added it to the text.

L176 : "Organized convection causes the insects to congregate due to the lower BL convergence related to the updraft zones. The number density of insects in the updraft zone is probably further increased by the insects' tendency to resist upward motion to lower temperatures, adiabatic cooling of the rising air." Please rephrase these two sentences. I think there are many ideas in there but need to be further explained. Personally, I don't know anything about insects and this is hard to link it to the dynamics you seemed to describe.

Answer: We made this part more concise.

"Insects tend to congregate at the updraft zones of rolls and they can be seen as clear air echoes by weather radars."

The point is that the weather radar can be used as an effective tool in detecting rolls, since insects are usually present in the air during the summer season.

L 225 : induced not induced

Answer: Fixed.

Figure 8 : These two figures are pretty interesting but I think that you need the reader to understand what you show. So here there are apparently 2 event types : One regional and one induced by roll vortices. Looking at Figure 5b, I see several zones associated with high N3-20. One in the 4 first km north to SMEAR II mast and the second one is further north (12km). According to wind speed direction the one located further north

did not cross the site measurement. So my question is how could you separate the Roll vortices induced NPF from the regional one given the fact that both are located in the same zone ? If you used only the mean geometrical diameter, could you please justify why this is relevant ???

Answer: We know that the high N3-20 zone 4 km north of SMEAR II moved over the station and over the zeppelin's measurement area from south-west to north-east, which is perpendicular to the mean wind direction. This is illustrated in Figure 3 where the location of each concentrated particle stripe observation is put onto a map. The dot size for the zeppelin measurements is proportional to the altitude.

In addition, analysis of wind components measured from the top of the 125 m mast confirms that the rolls were moving in the same direction and at a rate consistent with the RI-NPF observation in Figure 8 B (Figure 4). The rolls were also observed in the weather radar image as parallel lines of higher reflectance (Figure 5).

In Figure 4, vz, vâĹě and vâŁě refer to the vertical wind component, the wind component along the rolls (direction checked from weather radar) and the wind component perpendicular to rolls (positive direction to the left side of the parallel wind component). All components have a low-frequency peak at 4e-4 Hz and the phase differences are consistent with rolls moving to the north-east of the station (see the methods section on detection of roll vortices). 4e-4 Hz is consistent with one roll moving over the station in about 20 minutes.

From the airplane the high N3-20 zone 4 km north of SMEAR II was observed around 10:00 AM, just when it had moved over the field station. The particle region 12 km north of Hyytiälä was observed at the end of the flight (around 11:30 AM). Probably the RI-NPF event moved further north-east with the rolls during the measurement, or it could be that this is a new RI-NPF occurring in an adjacent roll or rolls that previously did not extend all the way to the measurement area. The roll vortices are not perfectly straight continuous structures and undergo change over time.

In Figure 8 the mean geometric diameters were fitted over the growing particle mode and then we chose the time periods when we were measuring the concentrated particle stripes (that is we were measuring the RI-NPF, where the regional NPF was enhanced) and when we were not measuring them (we were only measuring the regional NPF).

Interactive comment on Atmos. Chem. Phys. Discuss., https://doi.org/10.5194/acp-2019-1013, 2020.

Printer-friendly version

Discussion paper

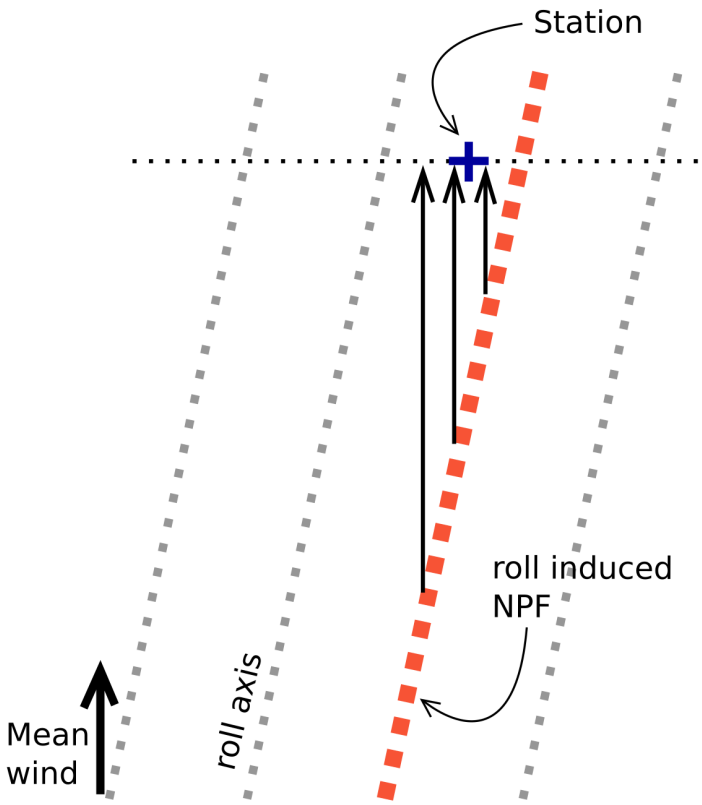

Fig. 1. An illustration of how a difference in the direction of the mean wind and the roll axis causes the rolls (and roll-induced NPF) to move over a stationary point perpendicular to the mean wind.

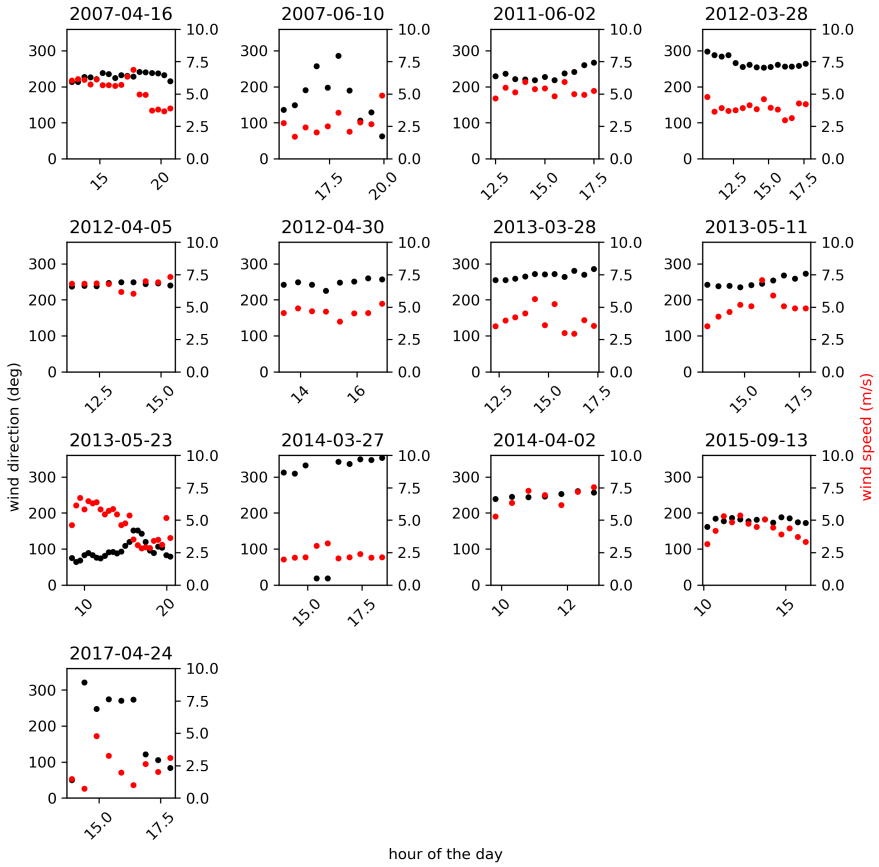
2007-04-16
2007-06-10
2011-06-02
2012-03-28
2012-04-05
2012-04-30
2013-03-28
2013-05-11
2013-05-23
2014-03-27
2014-04-02
2015-09-13
2017-04-24
wind direction (deg)
wind speed (m/s)
hour of the day

Fig. 2.

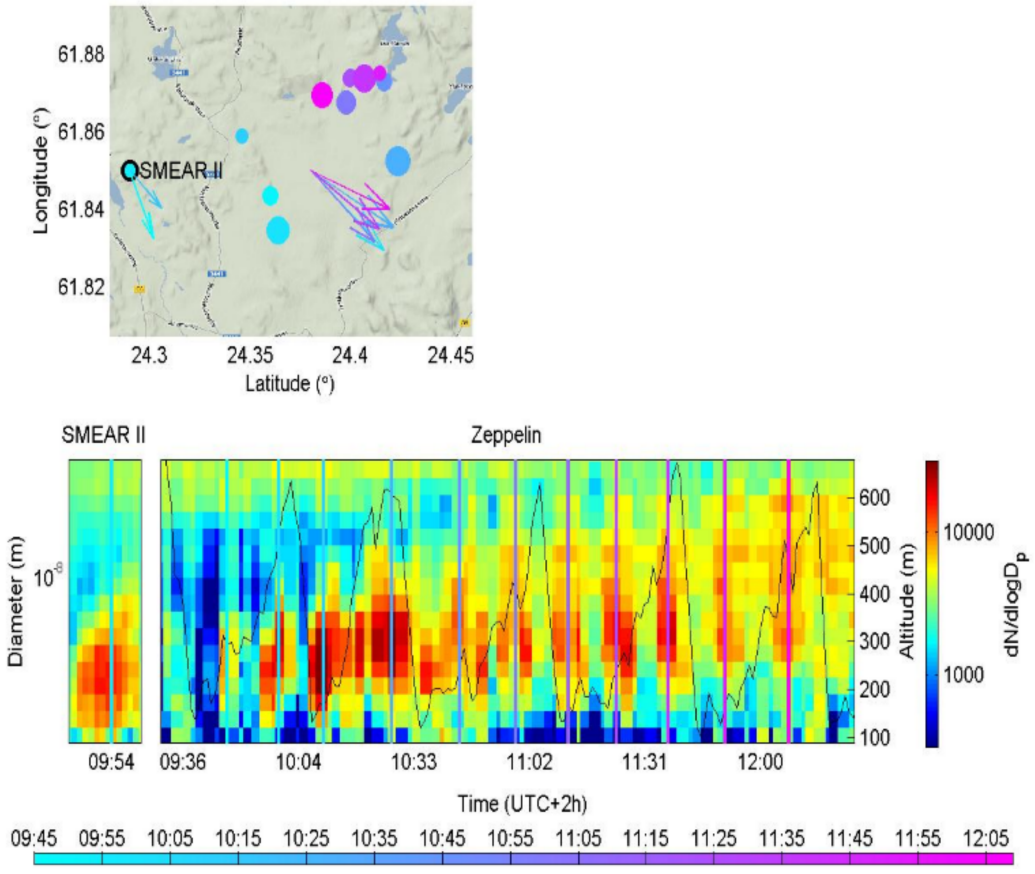
61.88
61.86
61.84
61.82
Longitude (°)
SMEAR II
24.3
24.35
24.4
24.45
Latitude (°)
SMEAR II
Zeppelin
Diameter (m)
10^-8
600
500
400
300
200
100
Altitude (m)
10000
1000
dN/dlogDp
09:54
09:36
10:04
10:33
11:02
11:31
12:00
Time (UTC+2h)
09:45 09:55 10:05 10:15 10:25 10:35 10:45 10:55 11:05 11:15 11:25 11:35 11:45 11:55 12:05

Fig. 3.

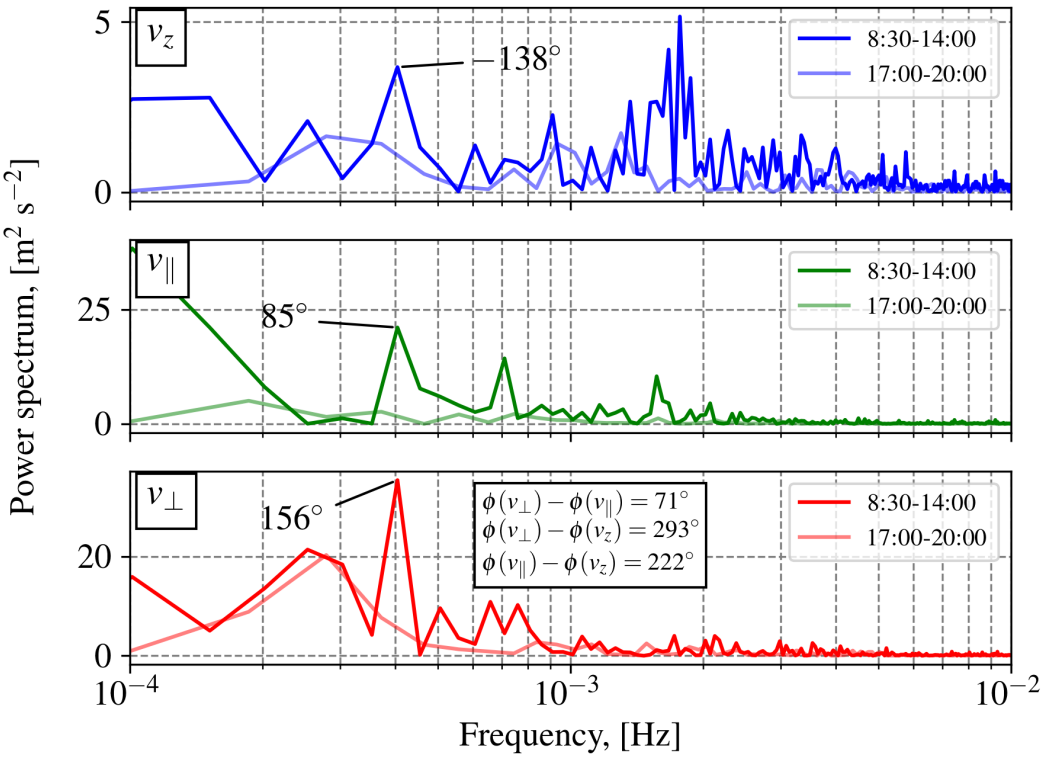
v_z
138°
8:30-14:00
17:00-20:00
$v_\parallel$
85°
8:30-14:00
17:00-20:00
$v_\perp$
156°
$\phi(v_\perp) - \phi(v_\parallel) = 71°$
$\phi(v_\perp) - \phi(v_z) = 293°$
$\phi(v_\parallel) - \phi(v_z) = 222°$
8:30-14:00
17:00-20:00
Power spectrum, [m^2 s^{-2}]
Frequency, [Hz]

Fig. 4.

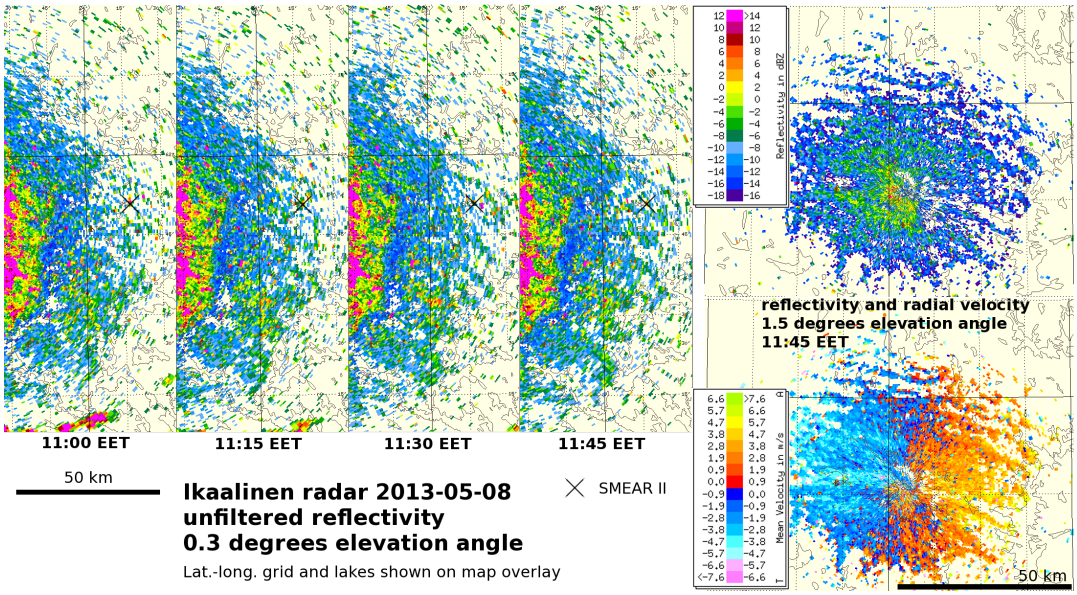
11:00 EET
11:15 EET
11:30 EET
11:45 EET
50 km
Ikaalinen radar 2013-05-08
unfiltered reflectivity
0.3 degrees elevation angle
Lat.-long. grid and lakes shown on map overlay
SMEAR II
reflectivity and radial velocity
1.5 degrees elevation angle
11:45 EET
50 km

Fig. 5.

Atmos. Chem. Phys. Discuss.,
https://doi.org/10.5194/acp-2019-1013-AC2, 2020

Atmospheric Chemistry and Physics Discussions

Interactive comment on "Roll vortices induce new particle formation bursts in the planetary boundary layer" *by* Janne Lampilahti et al.

Janne Lampilahti et al.

janne.lampilahti@helsinki.fi

Received and published: 7 July 2020

We thank the referee for the constructive comments, please find our responses below.

General Comments

This study presents evidence from field data of the formation of aerosol particles from volatile organic compounds (New Particle Formation, NPF) due to the transport of boreal forest air to the upper regions of the atmospheric boundary layer by the convective boundary layer rolls. This is a relevant topic that deserves to be studied and understood, since it can have direct impact on the estimation and modeling of aerosols in the atmosphere, which are relevant for air quality, weather and climate. This study presents a dataset that shows clear evidence of the relationship between convective rolls and

Printer-friendly version

Discussion paper

NPF. However, the manuscript needs some improvement in terms of the scientific writing. Due to its relevance, I suggest (1) improvements to the scientific presentation of the study, and (2) some additional analysis and discussion that can help future studies on the development of better measurements and models for this phenomenon.

Introduction: it is too short and some important information is lacking. For ex- ample, it needs more details on what is NPF (how it is defined, range of particle sizes of interest, where it comes from), why it is important (where it is used, where it is not used but should be used) and what are the mechanisms in which ABL dynamics might influence NPF. It would be important to describe in details what is already known about the relationship between NPF and convective rolls, what is not known (or never observed in field data), and what will be investigated here exactly. Why convective rolls, but not convective conditions in general? With this information the reader should be convinced about the relevance of this study. Right now this description (and consequently the motivation) of the study is su- perficial, only someone in the field will recognize its importance. It is important to convince the general audience as well. Some interesting information that should be in the intro is mentioned in the Conclusion section and in the caption of Figure 10.

Answer: we extended the first paragraph in the introduction to give more details on NPF. We moved the explanation on how roll vortices could induce NPF above the boreal forest from the conclusions to the introduction along with Figure 10. We made the the rest of the introduction mode detailed by following to the comments below.

Methods: the section already starts with “Zeppelin measurements”, without introducing the reader with the big picture of the methods of the study. It would be useful to start with a overall description (type of data, location, overall goal with each type of data, etc). After situating the reader, then go to the details. All the details needed to reproduce the analysis should be given. Some information is described in the results section (or in the caption of figures), some is missing (see details below). I’m very confused about the different particle size ranges mentioned in different moments of the manuscript. It

there a range of interest?

Answer: we added in the beginning a paragraph giving an overview of the measurements. In the detailed sections we took the below comments into account and rephrased or added text. In the conditions for roll-induced NPF we were looking at sub-20 nm particles, since this data was readily available from all measurement platforms.

Results: these results are very interesting, but they are too focused on the measurements of particles, but not on the atmospheric conditions. Maybe the gas and meteorological data at the surface could be used to provide quantitative information about the roll-induced NPF? It would be interesting to characterize the roll days with their micrometeorological variables, and to try to better identify the differences between the days with and without NPF. If this is not possible, it should be addressed in the manuscript, with a discussion of what should be done in future field studies in order to provide better quantitative data that can be used to model this phenomenon.

Answer: we agree that the analysis could be expanded. For example developing more comprehensive methods to measure the phenomenon and studying the cluster composition during roll-induced NPF. However we find this further analysis is beyond the scope of this study.

We added to the conclusions: “In order to fully understand roll-induced NPF, better measurement and analysis methods need to be developed. For example measuring the fluxes of sub-10 nm particles and doing airborne flux measurements. More measurements with a turbulence probe on board need to be performed. It would also be interesting to study the cluster composition during roll-induced NPF.”

Specific Comments

l. 25: “the small clusters and particles originating from these bursts grow in size similar to particles typically ascribed to regional scale atmospheric NPF”. The difference

between regional scale NPF and rolls induced NPF should be made clearer.

Answer: we rephrased the text to show the difference between roll-induced and regional scale NPF more clearly:

"the small clusters and particles originating from these localized bursts grow in size similar to particles typically ascribed to atmospheric NPF that occurs almost homogeneously at a regional scale."

l. 40: "In observational studies enhanced nucleation mode particle concentrations have been observed in turbulent layers in the lower atmosphere. For example inside the residual layer (Wehner et al., 2010) and in the inversion capping a shallow mixed layer (Platis et al., 2015; Siebert et al., 2004)." It is not clear how these two layers would favor the development of NPF, compared to other ABL conditions.

Answer: we added text explaining why BL dynamics can be important for NPF:

"Numerical studies have shown that fluctuations in ambient temperature and relative humidity, caused by for example small-scale turbulence, large eddies such as roll vortices (Easter and Peters, 1994), or mixing over a temperature inversion (Nilsson and Kulmala, 1998) can lead to significant enhancements in new particle formation rate compared to only mean conditions. This is because the formation rate has a nonlinear dependence on temperature and the gas-phase concentrations of the precursor vapors. Therefore, fluctuations in these variables, as opposed to mean conditions where the fluctuations are averaged out, can have a net enhancing effect on the source strength of aerosol particles by NPF."

Now it should be more clear why turbulence would favor NPF in these layers. We also edited the text a bit:

"In observational studies, increased nucleation mode particle concentrations have been measured in atmospheric layers where turbulent fluctuations were enhanced. For example in turbulent layers inside the residual layer (Wehner et al., 2010) and in

the inversion capping a shallow mixed layer (Platis et al., 2015; Siebert et al., 2004)."

l. 40: what is "nucleation mode particle"?

Answer: we added "sub-25 nm" to the text where we introduce NPF.

l. 43: "Other airborne measurements have found significant horizontal and vertical variability in the number concentration of nucleation mode particles within the BL." Can you expand on that? What level of variability? Anything measured within the ABL has variability, what makes this one worth pursuing?

Answer: we added text about the degree of variation that can be found

"Other airborne measurements have found that during NPF the number concentration of nucleation mode particles shows considerable, up to an order of magnitude, variation within the BL"

l. 49: "Convection in the planetary BL often organizes into counter-rotating horizontal roll vortices or rolls that extend to the top of the boundary layer". What is the horizontal and time scales of these rolls? How can they be identified by micrometeorological variables? This is relevant to evaluate if the measurements are appropriate. Why this specific type of convection is more relevant for NPF than others?

Answer: we added Figure 1 that shows 3d view of roll circulation with labels that explain the scale. The methods to identify roll vortices in the BL are outlined in the methods section. We also moved the explanation and the associated figure of the concept behind roll-induced NPF from the conclusions to the introduction.

l. 55: "and the overall effect of rolls on aerosol particle formation is unknown". Is it completely unknown? Can you be more specific on what is known, what is unknown? You have cited papers that discuss this.

Answer: we rephrased the text to be more specific

"However direct observations of the effects of roll vortices on NPF are lacking."

l. 68: “We used the positively charged particles and the data was averaged to 4 min time resolution”. Why? Is that equivalent to the total concentration of particles?

Answer: we modified the text to read

“We used the total particle data from the positive polarity of the instrument.”

In our case both polarities looked roughly the same in terms of data quality so the choice was more or less arbitrary, but in any case one should perform the analysis on one polarity only so that the data is most comparable.

l. 72: “The data was corrected for diffusional losses in the one meter long, 37 mm inner diameter, inlet tube and converted to standard conditions (293.15 K and 1 atm).” How? Can you provide at least a reference, so that someone could reproduce what was done exactly?

Answer: we added a reference to the diffusion loss calculation

“Gormley, P. G. and Kennedy, M.: Diffusion from a Stream Flowing through a Cylindrical Tube, Proc. R. Ir. Acad. Sect. Math. Phys. Sci., 52, 163–169, 1948.” We also added the equation for the conversion to standard conditions.

Sec 2.1: it is not clear after this section if the zeppelin data is only profiles or if there are measurements fixed at a given height.

Answer: we made the text more specific:

“The zeppelin measurements consisted of consecutive profiles. Each profile was a slow and even ascend (∼25 min) from ∼100 m up to ∼1 km above ground followed by a fast descend (∼5 min) while the speed relative to the surrounding air (airspeed) was kept at ∼20 m/s.”

l. 89: “Particle number concentration in the 3-20 nm range was calculated by subtracting the total particle number concentration measured by the Scanning Mobility Particle Sizer (SMPS) from the number concentration measured by the Ultrafine Condensation

Particle Counter (UCPC)." Not clear what that means. Why are you interested in this range only? The SMPS is mentioned in Table 1 as measuring between 10-400 nm. No information about UCPC is given. This description is not clear.

Answer: we modified the text

"We used the particle number concentration in the 3-20 nm size range as an indication of particles that likely originated from NPF. The 3-20 nm particle number concentration was calculated by subtracting the total particle number concentration measured by the Scanning Mobility Particle Sizer (SMPS) in the size range 20-400 nm from the number concentration measured by the Ultrafine Condensation Particle Counter (UCPC). We skipped the smallest size bins of the SMPS because they were in some cases noisy."

We also added UCPC in the Table 1.

l. 91: "The SMPS starts to lose accuracy in terms of spatial distribution of the aerosol particles due to its 2 min averaging period when the horizontal scale becomes less than 4 km." How does that apply to your study? Is this scale comparable to the phenomenon that you are investigating? Is this relevant? What about the other instruments used?

Answer: we decided to leave this part out because of the following reasons:

During the roll-induced NPF observations the number concentration from the UCPC was elevated during a large part of at least one SMPS scan. In these cases the SMPS total number concentration did not increase at all (the particles were below the detection limit) or the number concentration was momentarily (one or more SMPS scans) increased in the smallest size bins (10-20 nm) of the SMPS. An example is presented in Figure 2 where purple arrows show the times when the airplane flew through a roll-induced NPF.

In light of this we would say that the calculated 3-20 nm number concentration was in our cases a reliable indication that the number concentration was increased in the 3-20 size range. Therefore mentioning this limitation here is not relevant and can lead to

confusion.

l. 93: “A turbulence probe, capable of measuring the 3d wind vector, was only installed at the end of the 2015 campaign.” This sentence is completely lost here. What is this going to be used for? And how? Any details on this instrument? Measurement frequency, probe model, post processing?

Answer: we added the following paragraph:

“In order to detect roll vortices on board the airplane we installed a turbulence probe (Aventech Research, AIMMS-20) at the end of the 2015 campaign. The AIMMS-20 was capable of measuring the the 3d wind vector at 20 Hz, but for the analysis we averaged the data to 1 s.”

Sec 2.2: it is also not clear after this section if the airplane data used is only profiles or if there are measurements fixed at a given height.

Answer: we wrote the following:

“Typical measurement tracks consisted of ∼30 km long flight segments flown roughly perpendicular to the mean wind direction over the same area while doing a single vertical profile from 100 m to 3000 m above ground. The ascend and descend speeds were on average ∼1 m/s.”

l. 122: “The CPC had a 10 nm cutoff size” what is the measurement range? what is CPC?

Answer: the CPC measured all particles above 10 nm. We rephrased the text:

“The system measuring the vertical particle flux used an ultrasonic 3d anemometer combined with a condensation particle counter (CPC) at 23 m above ground. The CPC had a 10-nm cutoff size.”

l. 132: what is Aitken mode?

Answer: we added “Aitken mode (25-100 nm)”

Sec 2.4: Is there an exact quantitative criteria for NPF days, or was it selected by inspection only?

Answer: this is done by inspection, we added this to the text.

l. 147: What is the time interval used? What size ranges are used? How is the coagulation sink obtained? It is important to provide all information from the data to the results presented.

Answer: we added the following:

“We calculated the CoagSd from the DMPS data and for the number concentrations we used the NAIS data, so that the final time resolution of the formation rate was 4 min. The size ranges used from the NAIS data were 3-6 nm for J3 and 10-20 nm for J10.”

Sec. 2.8: I did not see the use of the ABL height in the results section.

Answer: in roll-induced NPF condition (i) we specify that the concentrated longitudinal sub-20 nm particle zone should be inside the BL and this is where we checked the BL height.

l. 193: “Figure 2 shows a frequent observation in the measurement data:” which data?

Answer: rephrased to “Figure 2 shows a frequent observation in the ground-based aerosol particle measurements”

Results section: why is the particle range size different in different analysis (for example figs 4 and 5, or between conditions (i) and (ii))

Answer: in the roll-induced NPF conditions (i) and (ii) we are looking at sub-20 nm particles.

We changed the size range in Figure 4 to be 3-20 nm instead of >1.5 nm in order to be consistent. In Fig. 5 the size range is also 3-20 nm.

In Figure 3 the SMPS stopped working in the middle of the flight, which is why we are only showing data from the UCPC (>3 nm). However, we know from the simultaneous ground-based observations that the observed particles were sub-20 nm.

l. 208-216: this paragraph should be in the Methods section.

Answer: we think it is necessary to explain the case study before defining the two roll-induced NPF conditions. Otherwise it is very difficult for the reader to understand why we define the conditions the way we do.

l. 228-229: which statistic test was performed? All information necessary to reproduce your results should be given.

Answer: the statistical test was Fisher's exact test. It is mentioned in the text.

l. 229-232: can you verify in the data what micrometeorology conditions characterize NPF and non-NPF days?

Answer: NPF events generally occur on sunny days with a lot of atmospheric mixing. Our data does agree with this (see Figure 3). However this figure adds little to understanding roll-induced NPF so we chose to leave it out of the manuscript.

l. 235: "This timescale is associated with mixing throughout the convective BL" did you calculate it? Compared with references?

Answer: we changed this sentence to be more specific to rolls: "This timescale is similar to the period of a typical roll vortex". A reference (Easter and Peters, 1994) was given in the introduction. This time scale is also similar to the mixing throughout the BL since the rolls circulate the air throughout the depth of the BL.

l. 238-244: instead of Table 3, it would be useful to show plots related to the estimation of GR. Also, what is the particle range size of your GR estimate?

Answer: we see that a good example of growing roll-induced NPF particles is already shown in Figure 8 where mean mode diameters are fitted to multiple subsequent roll-

induced NPF observations and over time they show a growth trend. We added fit lines and the resulting GRs to the figure also. For the GR estimate the median lower size was 7.5 nm and the median upper size was 15 nm. We added this information to the text.

Figure 8: "and power spectra of the wind components from the station's mast showed that the rolls were moving over the site" this would be interesting to see, maybe it could be added to this figure as a third panel?

Answer: the power spectra, along with two other supporting figures showing the movement of the roll-induced NPF and the rolls in the weather radar image, can be seen in our reply to Referee #1 (Fig. 4, explanation of the figure is in the answers). We find that the figure is quite technical and would not add significant extra value.

We made the description in the caption more precise:

"The roll-induced NPF event was moving over the measurement area from southwest to northeast. Weather radar observations showed that rolls were present over the measurement site and power spectra of the wind components from the station's mast showed that the rolls were moving over the site at the same rate (one roll in $\sim$20 min), and in the same direction as the roll-induced NPF."

The analysis in Figure 9 is not clear to me. It needs to be better explained in the methods and results section, not only in a figure caption. All the details needed to reproduce your results should be presented.

Answer: we added a detailed explanation to the text, see our answer to the first referee.

Figure 10 is more appropriate for the introduction than conclusion. A good de- scription of the physical process that motivates this study is in the caption of the figure, and it would be important for the reader to know about these things since the beginning.

Answer: we moved the figure to the introduction.

Technical Corrections

l. 40: “In observational studies, enhanced” (add the comma)

Answer: fixed

l. 52: “(Buzorius et al., 2001; Nilsson et al., 2001)” you don’t have to cite the same thing twice on the same sentence.

Answer: fixed

l. 55: “However direct observations (...)”, rephrase.

Answer: we rephrased this to “However direct observations of the effects of roll vortices on NPF are lacking.”

l. 67: what is “mobility diameter”?

Answer: the SMPS, DMPS and NAIS diameters are electrical mobility equivalent diameters. We decided to refer to simply diameters throughout the text to avoid confusion.

l. 79: “while the airspeed was kept at 20 m/s” not clear what that means

Answer: we modified the text to read “the speed relative to the surrounding air (airspeed) was kept at $\sim$20 m/s.”

Table captions: remove the word “Explanations:”

Answer: fixed

l. 85: Table 1 also mentions the Zepelin data, why is it mentioned only in the Airplane section?

Answer: we moved the sentence to the overview in the beginning of the methods section.

l. 96: “such that the aircraft was either descending, ascending or staying level”, maybe rephrase as “measurements performed during descending, ascending...”

Answer: rephrased

“Typical measurement tracks consisted of ∼30 km long flight segments flown roughly perpendicular to the mean wind direction over the same area while doing a single vertical profile from 100 m to 3000 m above ground (Figure 3). The ascend and descend speeds were ∼1 m/s.”

l. 98: “The measurement airspeed was 36 m/s”, again, not clear.

Answer: the airspeed is now explained in the Zeppelin section, so this should be clear.

It goes from section 2.4 to section 2.8

Answer: fixed

l. 143: why no equation number?

Answer: equation number added

l. 221: “station. Whereas” change to comma

Answer: changed

I don’t think Table 2 is necessary, the statistics are sufficient.

Answer: we agree that the detailed information presented is not necessary, so we removed the table and the references to it from the text.

l. 225: “roll-inducued”

Answer: fixed

Table 3: as Table 2, I don’t think this is necessary. It should be presented the statistics, but the information for each individual day is not necessary for the understanding of the study. If you decide to keep these tables, maybe put them in an appendix or supplemental material.

Answer: we agree and decided to remove Table 3 from the text. The important statistics

(average growth and formation rates) can be found in the text and the important figure derived from Table 3 is Figure 9.

l. 265: equation number

Answer: equation number added

Interactive comment on Atmos. Chem. Phys. Discuss., https://doi.org/10.5194/acp-2019-1013, 2020.

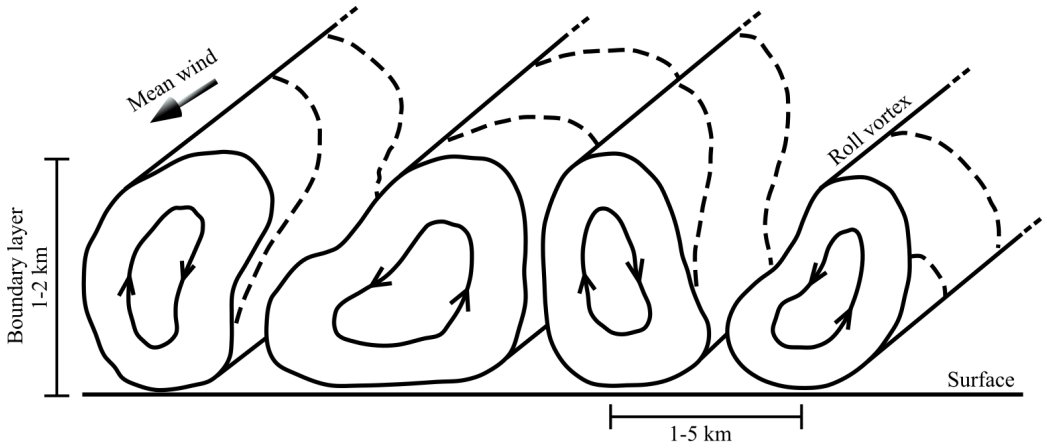

Fig. 1.

Printer-friendly version

Discussion paper

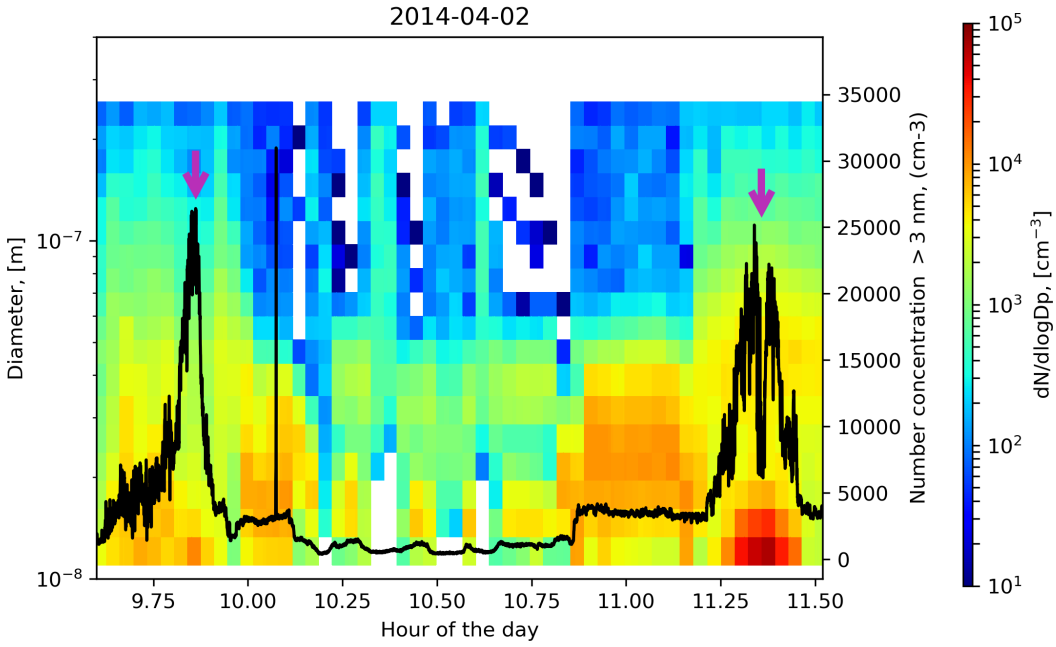
2014-04-02
Diameter, [m]
10^{-7}
10^{-8}
9.75
10.00
10.25
10.50
10.75
11.00
11.25
11.50
Hour of the day
35000
30000
25000
20000
15000
10000
5000
0
Number concentration > 3 nm, (cm-3)
10^{5}
10^{4}
10^{3}
10^{2}
10^{1}
dN/dlogDp, [cm^{-3}]

Fig. 2.

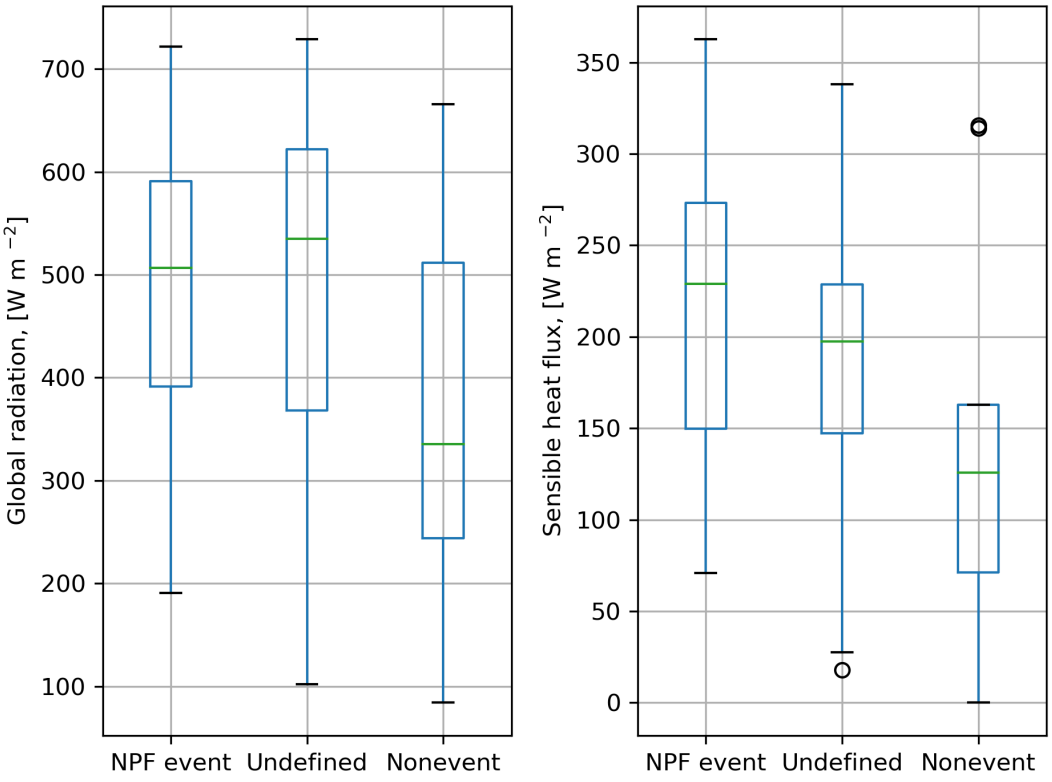
Global radiation, [W m $^{-2}$]
700
600
500
400
300
200
100
NPF event
Undefined
Nonevent
Sensible heat flux, [W m $^{-2}$]
350
300
250
200
150
100
50
0
NPF event
Undefined
Nonevent

Fig. 3.

Roll vortices induce new particle formation bursts in the planetary boundary layer

Janne Lampilahti[1], Hanna Elina Manninen[2], Katri Leino[1], Riikka Väänänen[1], Antti Manninen[3], Stephany Buenrostro Mazon[1], Tuomo Nieminen[1], Matti Leskinen[1], Joonas Enroth[1], Marja Bister[1], Sergej Zilitinkevich[1,3,4], Juha Kangasluoma[1,5], Heikki Järvinen[1], Veli-Matti Kerminen[1], Tuukka Petäjä[1,6], Markku Kulmala[1,5,6]

[1]Institute for Atmospheric and Earth System Research/Physics, Faculty of Science, University of Helsinki, Helsinki, Finland
[2]CERN, CH-1211 Geneva, Switzerland.
[3]Finnish Meteorological Institute, Helsinki, Finland.
[4]Department of Radio-physics, University of Nizhny, Novgorod, Russia.
[5]Aerosol and Haze Laboratory, Beijing Advanced Innovation Center for Soft Matter Science and Engineering, Beijing University of Chemical Technology, Beijing, China.
[6]Joint International Research Laboratory of Atmospheric and Earth System Sciences, Nanjing University, Nanjing, China.

Correspondence to: Janne Lampilahti (janne.lampilahti@helsinki.fi)

~~*Correspondence to*: Janne Lampilahti (janne.lampilahti@helsinki.fi)~~

Abstract. Recent studies have shown the importance of new particle formation (NPF) to global cloud condeensation nuclei (CCN) production, as well as to air pollution in megacities. In addition to the necessary presence of low-volatility vapors that can form the new aerosol particles, both numerical and observational studies have shown that the dynamics of the planetary boundary layer (BL) plays an important role in NPF. Evidence from field observations suggests that roll vortices might be favorable for inducing NPF in a convective BL. However, direct observations and estimates on the potential importance of this phenomenon to the production of new aerosol particles are lacking. Here we show that rolls frequently induce NPF bursts along the horizontal circulations, and that the small clusters and particles originating from these localized bursts grow in size similar to particles typically ascribed to atmospheric NPF that occurs almost homogeneously at a regional scale~~to regional-scale atmospheric NPF~~. We outline a method to identify roll-induced NPF from measurements and, based on the collected data, estimate the impact of roll vortices on the overall aerosol particle production due to NPF at a boreal forest site (83±34% and 26±8% overall enhancement in particle formation for 3-nm and 10-nm particles respectively). We conclude that the formation of roll vortices should be taken into account when estimating particle number budgets in the atmospheric BL.

1 Introduction

Atmospheric new particle formation (NPF) is a globally important source of aerosol particles and cloud condensation nuclei (CCN) (Dunne et al., 2016; Gordon et al., 2017; Kerminen et al., 2018; Kulmala et al., 2004), having potentially large influences on climate via aerosol-cloud interactions (Boucher et al., 2013) as well as on human health by increasing ultrafine particle number concentrations. NPF involves the formation of molecular clusters (~1.5 nm) in the atmosphere, and under specific conditions these clusters may grow to larger aerosol particles in the sub-100 nm size range. Under atmospheric background conditions, increased concentrations of nucleation mode (sub-25 nm) particles likely come from recent NPF. When the particles are larger than ~50 nm in diameter they can act as nuclei for cloud droplets (Kerminen et al., 2012) and influence radiative and other properties of clouds (e.g. Gryspeerdt et al., 2014; Rosenfeld et al., 2014).

Numerical studies have shown that fluctuations in ambient temperature and relative humidity, caused by for example small-scale turbulence, large eddies such as roll vortices (Easter and Peters, 1994), or mixing over a temperature inversion (Nilsson and Kulmala, 1998) can lead to significant enhancements in new particle formation rate compared to only mean conditions. This is because the formation rate has a non-linear dependence on temperature and the gas-phase concentrations of the precursor vapors. Therefore, fluctuations in these variables, as opposed to mean conditions where the fluctuations are averaged out, can have a net enhancing effect on the source strength of aerosol particles by NPF.

In observational studies, increased nucleation mode particle concentrations have been measured in atmospheric layers where turbulent fluctuations were enhanced. For example in turbulent layers inside the residual layer (Wehner et al., 2010) and in the inversion capping a shallow mixed layer (Platis et al., 2015; Siebert et al., 2004). Other airborne measurements have found that during NPF the number concentration of nucleation mode particles shows considerable, up to an order of magnitude, variation within the BL (Crumeyrolle et al., 2010; Leino et al., 2019; O'Dowd et al., 2009; Schobesberger et al., 2013; Väänänen et al., 2016). One possible reason for this could be the effect of BL dynamics.

Convection in the BL often organizes into counter-rotating horizontal roll vortices or rolls that extend to the top of the BL (Figure 1, e.g. Atkinson and Wu Zhang, 1996; Etling and Brown, 1993; Young et al., 2002). Buzorius et al. (2001) and Nilsson et al. (2001) noted that roll vortices commonly occurred during NPF events and suggested that they might be especially conducive to NPF.

For example, in the boreal forest the vegetation is an important source of volatile organic compounds that can be oxidized into low-volatile organic vapors (Ehn et al., 2014). Due to higher wind speeds the shear-generation of turbulence close to the vegetation is stronger in rolls than in cellular type convection (Zilitinkevich et al., 2006). Therefore, roll updrafts are particularly efficient at transporting vapors and molecular clusters from the surface to the top of the BL. On top of the BL decreased temperature, turbulence and mixing over the inversion layer can lead to a supersaturation of the vapors and activation of the clusters, leading to subsequent NPF (Easter and Peters, 1994; Nilsson and Kulmala, 1998). The newly-formed particles grow in size in the weaker and wider downdraft and end up close to the surface where they may be deposited on surfaces or continue growing while being transported in the air. These processes are illustrated in (Figure 2). The period for this sequence of processes is roughly an hour (Easter and Peters, 1994).

~~Atmospheric new particle formation (NPF) is a globally important source of aerosol particles and cloud condensation nuclei (CCN) (Dunne et al., 2016; Gordon et al., 2017; Kerminen et al., 2018; Kulmala et al., 2004), having potentially large influences on climate via aerosol-cloud interactions (Boucher et al.,~~

~~2013) as well as on human health by increasing ultrafine particle number concentrations. Numerical investigations have linked fluctuations in the ambient temperature and relative humidity, caused by for example small-scale turbulence, large eddies such as roll vortices, or mixing over a temperature inversion to significant enhancements in new particle formation rate compared to only mean conditions (Easter and Peters, 1994; Nilsson and Kulmala, 1998). In observational studies enhanced nucleation mode particle concentrations have been observed in turbulent layers in the lower atmosphere. For example inside the residual layer (Wehner et al., 2010) and in the inversion capping a shallow mixed layer (Platis et al., 2015; Siebert et al., 2004). Other airborne measurements have found significant horizontal and vertical variability in the number concentration of nucleation mode particles within the BL (Crumeyrolle et al., 2010; Leino et al., 2019; O'Dowd et al., 2009; Schobesberger et al., 2013; Väänänen et al., 2016). One possible reason for this could be the effect of BL dynamics.~~

~~Convection in the boundary layer of the atmosphere often organizes into counter-rotating horizontal roll vortices or rolls that extend to the top of the boundary layer (Atkinson and Wu Zhang, 1996; Etling and Brown, 1993; Young et al., 2002). Buzorius et al. (2001) and Nilsson et al. (2001) noted that roll vortices commonly occurred during NPF events and suggested that they might be especially inducive to NPF (Buzorius et al., 2001; Nilsson et al., 2001).~~

However direct observations of the effects of roll vortices on NPF are lacking. In this study we have analyzed co-located airborne and ground-based measurements from southern Finland during 2013-2015 in order to determine the effect of roll vortices on NPF.

~~However direct observations of roll vortices inducing NPF are lacking, and the overall effect of rolls on aerosol formation is unknown. In this study we have analyzed co-located airborne and ground-based measurements from southern Finland during 2013-2015 in order to determine the effect of roll vortices on NPF.~~

2 Methods

We analyzed data from airborne measurement campaigns conducted between 2013-2015 in southern Finland (see Table 1 for a summary of the airborne campaigns). These measurements had a general goal of measuring the vertical and horizontal distribution of aerosol particles in the lower atmosphere over a rural boreal forest area, with a special emphasis on NPF. The airborne observations were complemented by the continuous and comprehensive aerosol measurements at the SMEAR II station (Hari and Kulmala, 2005). The main tool to detect roll vortices was a nearby weather radar. Also wind data from the airborne and ground-based measurements was used.

2.1 Zeppelin measurements.

In May-June 2013, in the framework of the PEGASOS (Pan-European Gas-AeroSOls Climate Interaction Study) project, aerosol particle and gas phase measurements were performed over Hyytiälä and Jämi in southern Finland using an instrumented Zeppelin NT (Neue Technologie) airship.

~~In May-June 2013, in the framework of the PEGASOS (Pan-European Gas-AeroSOls Climate Interaction Study) project, aerosol particle and gas phase measurements were performed over Hyytiälä and Jämi in southern Finland using an instrumented Zeppelin NT (Neue Technologie) airship.~~

Here we analyzed measurements from the onboard nNeutral cluster and aAir iIon sSpectrometer (NAIS) (Mirme et al., 2010; Mirme and Mirme, 2013) on May 8, 2013. The NAIS measured ~~can measure~~ the particle number-size distribution in the ~~mobility~~ diameter range 2-42 nm and ion number-size distribution in the ~~mobility~~ diameter range 0.8-42 nm at 4 min time resolution. We used the total particle data from the positive polarity of the instrument~~the positively charged particles and the data was averaged to 4 min time resolution~~.

During the measurement the inlet of the NAIS was pushed out from the window of the zeppelin's gondola. The data was corrected for diffusional losses in the one meter long, 37 mm inner diameter, inlet tube (Gormley and Kennedy, 1948) and converted to standard conditions (293.15 K and 1 atm) using Equation 1, which can be derived using the ideal gas law:

$$N_{\mathrm{std}} = \left(\frac{1\,\mathrm{atm} \times T}{293.15\,\mathrm{K} \times p} \right) \times N \qquad (1)$$

where N refers to number concentration, T to temperature and p to pressure. The temperature and pressure recorded by the instrument were used in the corrections. Any losses occurring at the inlet nozzle were assumed to be negligible due small size of the measured particles and relatively low airspeed, so that the particles closely followed streamlines.

~~During the measurement the inlet of the NAIS was pushed out from the window of the zeppelin's gondola. The data was corrected for diffusional losses in the one meter long, 37 mm inner diameter, inlet tube and converted to standard conditions (293.15 K and 1 atm). The temperature and pressure recorded by the instrument were used in the corrections. Any losses occurring at the inlet nozzle were assumed to be negligible due small size of the measured particles and relatively low airspeed, so that the particles closely followed streamlines.~~

The zeppelin measurements consisted of consecutive profiles. Each profile was a s~~were helix-shaped with s~~low and even ascend~~s~~ (~25 min) from ~100 m up to ~1 km ~~height~~ above ground followed by a

fast d ~~and fast d~~escend~~s~~ (~5 min) while the speed relative to the surrounding air (airspeed)~~airspeed~~ was kept at ~20 m/s. The vertical profiles were flown over the same circular area that was only ~4 km in diameter (see Figure 3~~1~~). The flights started and ended at the Jämi airfield (61°46′43″N, 22°42′58″E, 154 m above sea level).

2.2 Airplane measurements

The University of Helsinki has organized several airborne measurement campaigns around Hyytiälä using an instrumented Cessna 172 airplane. Descriptions of the measurement setups can be found in previous studies (Leino et al., 2019; Schobesberger et al., 2013; Väänänen et al., 2016).

We used the particle number concentration in the 3-20 nm size range as an indication of particles that likely originated from NPF. The 3-20 nm particle number concentration was calculated by subtracting the total particle number concentration measured by the scanning mobility particle sizer (SMPS) in the size range 20-400 nm from the number concentration measured by the ultrafine condensation particle counter (UCPC). We skipped the smallest size bins of the SMPS because they were in some cases noisy.

In order to detect roll vortices on board the airplane we installed a turbulence probe (Aventech Research, AIMMS-20) at the end of the 2015 campaign. The AIMMS-20 was capable of measuring the the 3d wind vector at 20 Hz, but for the analysis we averaged the data to 1 s.

~~The University of Helsinki has organized several airborne measurement campaigns around Hyytiälä using an instrumented Cessna 172 airplane. Descriptions of the measurement setups can be found in previous works (Leino et al., 2019; Schobesberger et al., 2013; Väänänen et al., 2016). Table 1 shows a summary of the airborne measurement campaigns and the instrumentation from which data was used in this study.~~

Typical measurement tracks consisted of ~30 km long flight segments flown roughly perpendicular to the mean wind direction over the same area while doing a single vertical profile from 100 m to 3000 m above ground (Figure 3). The ascend and descend speeds were ~1 m/s. The measurement airspeed was 36 m/s. Usually two 2.5 h flights were flown during a single day, one in the morning and one in the afternoon. Vertically the measurements covered all parts of the BL as well as the lowest kilometer of the free troposphere. The flights started and ended at the Tampere-Pirkkala airport (61°24′55″N, 23°35′16″E, 119 m above sea level).

~~Particle number concentration in the 3-20 nm range was calculated by subtracting the total particle number concentration measured by the Scanning Mobility Particle Sizer (SMPS) from the number concentration measured by the Ultrafine Condensation Particle Counter (UCPC). The SMPS starts to lose accuracy in terms of spatial distribution of the aerosol particles due to its 2 min averaging period~~

~~when the horizontal scale becomes less than 4 km. A turbulence probe, capable of measuring the 3d wind vector, was only installed at the end of the 2015 campaign.~~

~~Typical measurement tracks consisted of ~30 km long flight segments flown roughly perpendicular to the mean wind direction over the same area such that the aircraft was either descending, ascending or staying level. The altitude range was between 100-3000 m above ground. The measurement airspeed was 36 m/s. Usually two 2.5 h flights were flown during a single day, one in the morning and one in the afternoon. Vertically the measurements were able to probe all parts of the BL as well as the lowest kilometer of the free troposphere. The flights started and ended at the Tampere-Pirkkala airport (61°24′55″N, 23°35′16″E, 119 m above sea level).~~

2.3 Ground-based measurements

The airborne measurements were complemented by the measurements at the SMEAR II field station. The measurement station is located in Hyytiälä, Finland (61°50'40"N, 24°17'13"E, 180 m above sea level) and is surrounded by flat terrain and coniferous forest. The station represents the background conditions found in the boreal forest regions of northern latitudes (Hari and Kulmala, 2005).

The key aerosol instruments included in this study were the station's differential mobility particle sizer (DMPS) (Aalto et al., 2001), the NAIS (Manninen et al., 2009) and the particle size magnifier (PSM) (Vanhanen et al., 2011). The time resolutions of the DMPS and the NAIS were 10 min and 4 min respectively, from the NAIS we again used particle data from the positive polarity. The DMPS measured the particle number-size distribution in the size range 3-1000 nm. The PSM measured particle number-size distribution between 1 and 2 nm and the time resolution was 12 min. The DMPS sampled the air from a vertical inlet at 8 m above the ground and the NAIS through a wall inlet at 2 m above the ground, both were inside the canopy. The PSM was sampling in a 35-m tall tower, above the forest canopy. The aerosol particle data from the station was not converted to standard conditions since the correction would be negligible.

~~The key aerosol instruments included in this study were the station's Differential Mobility Particle Sizer (DMPS) (Aalto et al., 2001), the NAIS (Manninen et al., 2009) and the Particle Size Magnifier (PSM) (Vanhanen et al., 2011). From the NAIS the positively charged particles were used and the data was averaged to 4 min time resolution. The PSM measured particle number-size distribution between 1-2 nm and the data was averaged to 12 min time resolution. The DMPS sampled the air from a vertical inlet at 8 m above the ground and the NAIS through a wall inlet at 2 m above the ground, both were inside the canopy. The PSM was sampling in a 35 m tall tower, above the forest canopy. The aerosol particle data from the station was not converted to standard conditions since the correction would be negligible.~~

Measurements of meteorological variables (temperature, relative humidity, wind direction and speed) and vertical particle flux from the station's mast (at 33.6 m above ground) were available at 1-min and 30-min time resolution respectively. The meteorological variables were measured at 33.6 m above ground. The system measuring the vertical particle flux used an ultrasonic 3d anemometer combined with a condensation particle counter (CPC)~~CPC~~ at 23 m above ground. The CPC had a 10-nm cutoff size. The vertical particle flux was calculated using the eddy covariance method (Buzorius et al., 2000)~~. Wind data was also used from an ultrasonic 3d anemometer that was situated at 125 m above ground on top of the station's mast~~.

2.4 NPF event analysis

NPF event analysis, as described by Kulmala et al. (2012), was done for the flight measurement days. First the measurement days were classified by visual inspection into three different NPF event classes (NPF event days, undefined days and nonevent days) based on the DMPS data. NPF event days display a continuously and smoothly growing particle mode starting from the smallest detectable size. This indicates a regional NPF event. On undefined days sub-25 nm particles are only intermittently (less than an hour) observed without apparent growth or a growing Aitken mode (25-100 nm) appears, possibly arising from a NPF episode elsewhere. On nonevent days no increase in sub-25 nm particle number concentration is observed.

~~NPF event analysis, as described by Kulmala et al. (2012), was done for the flight measurement days (Kulmala et al., 2012). First the measurement days were classified into three different NPF event classes (NPF event days, undefined days and nonevent days) based on the DMPS data. NPF event days display a continuously and smoothly growing particle mode starting from the smallest detectable size. This indicates a regional NPF event. On undefined days sub-25 nm particles are only intermittently observed without apparent growth or a growing Aitken mode appears, possibly arising from a NPF episode elsewhere. On nonevent days no increase in sub-25 nm particle number concentration is observed.~~

Particle growth rate (GR) is the rate of change of particle diameter. We used the so-called mode-fitting method to determine the particle GRs. The method involves fitting log-normal curves over the particle size distributions on the growing particle mode, defining the peaks as the geometric me~~me~~an particle diameters of the mode, and then using the change in the geometric mean~~mean particle~~ diameter with respect to time to calculate the GR.

The formation rate of particles of the diameter d is defined as the rate at which the freshly-formed particles enter the size range $[d, d + \Delta d]$ as a result of their formation and growth. The formation rate J_d was calculated using the following equation (Kulmala et al., 2012):

~~The formation rate of diameter d particles is defined as the rate at which the freshly formed particles enter a certain size as a result of NPF. The formation rate J_d was calculated using the below formula (Kulmala et al., 2012)~~

$$\frac{dN_d}{dt} = J_d - \frac{GR}{\Delta d} \times N_d - CoagS_d \times N_d \qquad (2)$$

where N_d is the number concentration of particles in the size range $[d, d + \Delta d]$, GR is the growth rate and $CoagS_d$ is the coagulation sink for the particles in the size range. We calculated the $CoagS_d$ from the DMPS data and for the number concentrations we used NAIS data, so that the final time resolution of the formation rate was 4 min. The size ranges used from the NAIS data were 3-6 nm for J_3 and 10-20 nm for J_{10}.

~~where N_d is the number concentration of particles in the size range Δd, GR is the growth rate and $CoagS_d$ is the coagulation sink for the particles in the size range.~~

2.~~5~~8 Determination of BL height.

The height of the BL was determined from the aircraft measurements by inspecting the vertical profiles of relative humidity and potential temperature. The purpose was to determine if the roll-induced NPF events were observed inside the BL or above it.

We used two of the methods outlined by Seidel et al., (2010). The height of the BL was determined to be approximately at the altitude where there was a minimum vertical gradient in relative humidity and a maximum vertical gradient in potential temperature.

~~We used two of the methods outlined by Seidel et al. (2009) (Seidel et al., 2010). The height of the BL was determined to be approximately at the altitude where there was a minimum vertical gradient in relative humidity and a maximum vertical gradient in potential temperature.~~

2.~~6~~9 Detection of roll vortices

Inspecting satellite images for cloud streets was one way to deduce the presence of rolls (Etling and Brown, 1993). For this NASA's WorldView online tool was used. One limitation of this method was that clear sky rolls or rolls underneath a cloud cover could not be identified. Also the measurement flight time and the time of the satellite image were often separated by several hours and the meteorological conditions could change during that time.

The roll-axis can deviate from the mean BL flow direction (Miura, 1986) which causes the rolls to slowly move perpendicular to the mean BL flow direction, leaving low-frequency periodic variation in the time series of the wind components when measured from a stationary point (Buzorius et al., 2001; Smedman, 1991). This provided us with one way to determine if roll circulation was taking place. The

vertical and parallel to roll-axis wind components would always be in phase opposition while the phases of the perpendicular to roll-axis and parallel to roll-axis wind components would be separated by either 90 or -90 degrees depending on the direction of the roll movement (Brooks and Rogers, 1997; Vandemark et al., 2001). ~~We used the mean horizontal wind component in place of the parallel to roll-axis wind component since they should not deviate that much from each other.~~ The ~~roll-induced~~ variation in wind due to rolls could be directly observed in the smoothed wind components measured on board the airplane by the turbulence probe.

Insects tend to congregate at the updraft zones of rolls and they can be seen as clear air echoes by weather radars (Wainwright et al., 2017; Wilson et al., 1994). In our case the Finnish Meteorological Institute's C-band (5.6 GHz) weather radar in Ikaalinen (61°46'1.6"N, 23°4'47.6"E, 154 m above sea level) provided information on the existence and location of planetary BL rolls. The analysis of the radar data was based on the processed radar imagery. Most of the flight-tracks were in the range 50 to 70 km from the radar, and during the summer season insects are usually abundant enough to let the rolls be visible in the radar images over the area of airborne observations. The spatial resolution of the radar measurements is set by the antenna beam width and pulse duration. The Ikaalinen radar's resolution in the measurement range was 500 m, and the 1.0 degree beam gets about 1 km wide over the target area. Some small rolls may get unresolvable, because of the radar resolution, but more probably the detection would have been limited already by the weakness of the circulation of these tiny rolls to get enough insects airborne high enough.

~~Weather radars can detect clear air echoes, and insects are the most important source of echoes at these radio frequencies (Finnish C-band weather radars operate at 5.6 GHz) (Wainwright et al., 2017; Wilson et al., 1994). The lack of insects in the air limits the important period of the use of weather radar clear air echoes in Finland approximately from May to September. Organized convection causes the insects to congregate due to the lower BL convergence related to the updraft zones. The number density of insects in the updraft zone is probably further increased by the insects' tendency to resist upward motion to lower temperatures, adiabatic cooling of the rising air. As a result the weather radars show the maxima of upward motions as maxima of reflectivity (Wainwright et al., 2017).~~

~~In our case the Finnish Meteorological Institute weather radar in Ikaalinen (61°46'1.6"N, 23°4'47.6"E, 154 m above sea level) provided information on the existence and location of planetary BL rolls. The analysis of the radar data was based on the processed radar imagery. Most of the flight-tracks were in the range 50 to 70 km from the radar, and during the summer season insects are usually abundant enough to let the rolls be visible in the radar images over the area of airborne observations. The spatial resolution of the radar measurements is set by the antenna beamwidth and pulse duration. Ikaalinen~~

~~radar resolution in range was 500 m, and the 1.0 degrees beam gets about 1 km wide over the target area. Some small rolls may get unresolvable, because of the radar resolution, but more probably the detection would have been limited already by the weakness of the circulation of these tiny rolls to get enough insects airborne high enough.~~

3 Results and discussion

Figure 4 shows a frequent observation in the ground-based aerosol particle measurements: a momentary increase in the number concentration of freshly formed clusters and aerosol particles during daytime, coupled with a relatively large fluctuation in the vertical particle flux. In Figure 4 the freshly formed clusters and aerosol particles were observed between 10:00 and 12:00.

Concurrent airplane measurements flown over the measurement station on that day (Figure 5) showed that the location of increased aerosol particle number concentration was directly on top of the SMEAR II station. The increased number concentrations were observed over multiple overpasses indicating that the concentrated zone was elongated along the mean wind direction. The vertical wind speed measurements on board the airplane revealed the presence of rolls as regularly alternating up- and downdrafts that were approximately aligned with the mean wind. The maximum number concentrations occurred in two adjacent roll downdrafts. Increased number concentrations were not observed above the BL, no pollution sources were close-by and the sky was cloudless.

~~Figure 2 shows a frequent observation in the measurement data: a momentary increase in the number concentration of freshly formed clusters and aerosol particles during daytime, coupled with a relatively large fluctuation in the vertical particle flux. Concurrent airplane measurements flown over the measurement station on that day showed that the location of increased aerosol particle number concentration was elongated along the mean wind direction, and that the maximum number concentrations occurred in two neighboring roll downdrafts (Figure 3). Increased number concentrations were not observed above the BL, no pollution sources were close-by and the sky was cloudless.~~

Wind measurements from the mast of the measurement station (Figure 6) showed that roll vortices were slowly moving perpendicular to the mean wind (this is due to a slight difference in the directions of the mean wind and the roll axis, see Figure 7 for an illustration). The periodic anti-correlation between the horizontal and the vertical wind components is a clear indication of roll vortices drifting over the measurement location perpendicular to the mean wind direction. This explains why particles were observed only momentarily at the field station, they were connected to specific rolls that drifted over the station. Overall, the observations on this day show that the roll circulation was locally inducing the formation of new aerosol particles.

In Figure 6 one observes that the fluctuations in vertical particle flux do not match the fluctuations in vertical wind due to rolls. This is likely because of the following reason. During a sunny August day with moderate wind, turbulence dominates vertical transport close to the canopy, so the variations in particle number concentration and vertical particle flux close to the canopy are decoupled from the roll circulation. When the roll-induced NPF first moves over the field site the number concentration above the turbulent layer increases and the particles start to mix downwards. Inside the turbulent layer the particle flux becomes negative and the number concentration starts to increase. As more and more particles are mixed downwards, the number concentration increases inside the turbulent layer while the particle flux becomes less negative. As the roll-induced NPF moves away, the vertical particle flux can become positive if the number concentration below the flux measurement becomes higher than the number concentration above.

We defined two conditions to identify roll-induced NPF from the measurement data. Condition (i): a roughly 1-5 km wide region of increased sub-20 nm particle number concentration was observed on the flight track during consecutive overpasses when the airplane was flying perpendicular to the mean wind direction inside the BL. This implies a long and narrow region of freshly formed particles inside the BL that is roughly aligned with the mean wind (see Figure 8 for examples). Condition (ii): in the ground-based measurements the number concentration of sub-20 nm particles momentarily (lasting between 0.5-2 hours) increased, and this increase was associated with opposite fluctuations in the vertical particle flux (see Figure 9 for examples). This would be due to the roll-induced NPF moving over the measurement station and it requires that the rolls are not aligned with the mean BL flow.

The roll-induced NPF condition (ii) never occurred at the same time without condition (i) being also true, but condition (i) did occur without condition (ii). This is likely because when the rolls were not aligned with the mean wind the roll-induced NPF could be observed from the airplane as well as from the station, whereas if the rolls were aligned with the mean wind, then the roll-induced NPF could still be observed from the airplane but not from the measurement station.

~~Wind measurements from the mast of the measurement station (Figure 4) showed that roll vortices were slowly moving perpendicular to the mean wind (this is due to a slight difference in the directions of the mean wind and the roll axis). This explains why particles were observed only momentarily at the field station, they were connected to specific rolls that drifted over the station. Overall, the observations on this day show that the roll circulation was locally inducing the formation of new aerosol particles.~~

The airborne measurement data was classified with respect to NPF events and for the presence of roll vortices and roll-induced NPF. Roll-induced NPF was observed on 30% (6/20) of the regional NPF event days and on 22% (8/36) of the days classified as undefined (Figure 10A). According to radar and

satellite observations the counter-rotating horizontal circulations were always present during the roll-induced NPF (Figure 10B) and according to Fisher's exact test this association was statistically significant (p=0.03). Roll vortices do not guarantee that roll-induced NPF occurs, since many other factors, such as a sufficient amount of sunlight and low enough sinks for low-volatile vapors and small clusters, are also important in determining whether atmospheric NPF may occur or not (Dada et al., 2017; Hamed et al., 2007).

~~We used two conditions to identify roll-induced NPF from the measurement data. Condition (i): a roughly 1-5 km wide region of increased sub-20 nm particle number concentration was observed on the flight track during consecutive overpasses when the airplane was flying perpendicular to the mean wind direction inside the BL. In other words this implies a long and narrow region of freshly formed particles inside the BL that is roughly aligned with the mean wind (see Figure 5 for examples). Condition (ii): in the ground-based measurements the number concentration of sub-20 nm particles momentarily (lasting between 0.5-2 hours) increased, and this increase was associated with opposite fluctuations in the vertical particle flux (see Figure 6 for examples). This would be due to the roll-induced NPF moving over the measurement station and it requires that the rolls are not aligned with the mean BL flow.~~

The timescale that a roll-induced NPF moves over the measurement station is roughly an hour. This timescale is similar to the period of a typical roll vortex and it allows us to estimate the total effect of a roll on NPF. Using condition (ii), we identified some of the clearest cases of roll-induced NPF (29 days and 46 roll-induced NPF events) from only the ground-based measurements during 2006-2017.

Multiple roll-induced NPF events during a single day were observed on 13/29 days. In these cases by looking at the change in particle diameter between subsequent roll-induced NPF events we were able to estimate the GR. In addition, on May 8, 2013 we could calculate the *GR* from a single roll-induced NPF event by following it with the zeppelin aircraft (Figure 11). We found that the median GR of the roll-induced NPF particles was 1.9 (inter quartile range (IQR) = 1.3-2.1) nm/h. The median size range for the GR estimation was 7.5-15 nm. This is similar to the median GR of 2.5 nm/h for 3-25 nm particles reported by Nieminen et al., (2014) for regional-scale NPF events observed at the station.

~~During the airborne measurement campaigns condition (ii) never occurred at the same time without condition (i) being also true, but condition (i) did occur without condition (ii). This is likely because when the rolls were not aligned with the mean wind the roll-induced NPF could be observed from the airplane as well as from the station. Whereas if the rolls were aligned with the mean wind, then the roll-induced NPF could still be observed from the airplane but not from the measurement station.~~

We aggregated all the roll-induced NPF observations into 1-hour-averaged bins using the median GR and the geometric mean diameters of the particles, assuming that the particles were formed at *t=0* hours (Figure 12).

Then we calculated the formation rates and their uncertainties. We assumed that the roll-induced NPF GRs were normally distributed with mean equal to the median GR and standard deviation given by the magnitude of the IQR. We randomly sampled a GR from the distribution and distributed the roll-induced NPF observations into 1-hour bins. For each 1-hour bin we assumed that the number-size distributions again followed a normal distribution with mean equal to the median and standard deviation given by the IQR. We randomly sampled a number-size distribution from each bin and calculated the formation rates based on that. We repeated this procedure 1000 times in order to estimate the J_3 and J_{10} and their uncertainties shown in Figure 12.

The resulting peak formation rate was 2.4 (IQR=1.6-3.1) $cm^{-3}s^{-1}$ for 3-nm particles and 0.4 (IQR = 0.2-0.6) $cm^{-3}s^{-1}$ for 10-nm particles. Nieminen et al., (2014) found that for regional-scale NPF events during springtime, the median formation rates of 3-nm and 10-nm particles were 1.0 cm^{-3} s^{-1} and 0.52 cm^{-3} s^{-1}, respectively.

In addition, we estimated the fraction of area covered by the roll-induced NPF. We assumed that the roll-induced NPF events extend much longer along the rolls, which is supported by the aircraft data. This means that for the area fraction we need to estimate what the spacing of the roll-induced NPF events is perpendicular to the direction of the rolls.

If the wind conditions stay the same during the period when the multiple roll-induced NPF events move over the station, then we can assume that the rolls move over the station at a steady pace. This means that dividing the time that subsequent roll-induced NPF events observed during the same day spent on top of the measurement station by the total time it took for the roll-induced NPF events to move over the site can be used as an area fraction estimate. According to measurements from the mast, on average the wind conditions during the observations did not change significantly.

We found that the fraction of area covered by the roll-induced NPF was 0.46 (IQR = 0.39-0.64). The roll systems are regionally roughly homogeneous (as demonstrated by cloud streets caused by the rolls in satellite images), so we can assume that the fraction of area covered by the roll-induced NPF events applies regionally and the phenomena is not limited to the close vicinity of the site.

~~The airborne measurement data was classifed with respect to NPF events and for the presence of roll vortices and roll-indeued NPF. The results are presented in Table 2. Roll-induced NPF was observed on~~

30% (6/20) of the regional NPF event days and on 22% (8/36) of the days classified as undefined (Figure 7A). According to radar and satellite observations the counter-rotating horizontal circulations were always present during the roll-induced NPF (Figure 7B) and this association was statistically significant (p=0.03). Roll vortices do not guarantee that roll-induced NPF occurs, since many other factors, such as a sufficient amount of sunlight and low enough sinks for low-volatile vapors and small clusters, are also important in determining whether atmospheric NPF may occur or not (Dada et al., 2017; Hamed et al., 2007).

The timescale that a roll-induced NPF moves over the measurement station is roughly an hour (see Table 3). This timescale is associated with mixing throughout the convective BL and it allows us to estimate the total effect of a roll on NPF. Using condition (ii), we identified some of the clearest cases of roll-induced NPF (29 days and 46 roll-induced NPF events) from only the ground-based measurements during 2006-2017 and summarized the results in Table 3. By looking at the change in particle diameter between subsequent roll-induced NPF events during the same day we found that the median *GR* of the roll-induced NPF particles was 1.9 (inter quartile range (IQR) = 1.3-2.1) nm/h. On May 8, 2013 we could calculate the *GR* from a single roll-induced NPF event by following it with the zeppelin aircraft (Figure 8). This is similar to the median *GR* of 2.5 nm/h for 3-25 nm particles reported by Nieminen et al. (2014) for regional-scale NPF events observed at the station (Nieminen et al., 2014).

We aggregated all the roll-induced NPF observations in Table 3 into 1-hour-averaged bins (Figure 9) using the median GR and the geometric mean diameters of the particles. This was used in the calculation of particle formation rates. The resulting peak formation rate was 2.4 (IQR=1.6-3.1) $cm^{-3}s^{-1}$ for 3-nm particles and 0.4 (IQR = 0.2-0.6) $cm^{-3}s^{-1}$ for 10-nm particles. Nieminen et al. (2014) found that for regional-scale NPF events during springtime, the median formation rates of 3-nm and 10-nm particles were 1.0 $cm^{-3}s^{-1}$ and 0.52 $cm^{-3}s^{-1}$, respectively (Nieminen et al., 2014).

In addition, we estimated the fraction of area covered by the roll-induced NPF by dividing the time that the subsequent roll-induced NPF events observed during one day spent on top of the measurement station with the total time it took for the roll-induced NPF events to move over the site. We found that the fraction of area covered by the roll-induced NPF was 0.46 (IQR = 0.39-0.64). The roll systems are regionally roughly homogeneous (as demonstrated by cloud streets caused by the rolls in satellite images), so we can assume that the fraction of area covered by the roll-induced NPF events applies regionally and the phenomena is not limited to the close vicinity of the site.

We combined the median formation rates, the median area coverage and the statistics obtained from the aircraft campaigns and estimated using Equation 3 ~~to estimate~~ how much, in terms of percentage increase, the roll-induced NPF enhances the production of new aerosol particles in Hyytiälä.~~:~~

$$J_d \text{ enhancement} = \frac{A(\text{roll-induced}) \times n(\text{roll-induced}) \times J_d(\text{roll-induced})}{n(\text{regional}) \times J_d(\text{regional})} \times 100\,\%. \qquad (3)$$

Here, *A* ~~where *a*~~ is the median area fraction ~~of the roll-indeued NPF~~, *n* is the number of roll-induced and regional NPF events observed and J_d is the median formation rate of particles at the diameter~~size~~ *d*. The uncertainty was calculated by using the propagation of uncertainty. We estimate that compared with only regional NPF, the roll-induced NPF enhances the production of new aerosol particles by 83±34% and 26±8% for 3-nm and 10-nm particles respectively. In addition to the enhancement of regional NPF, there were several days during which practically no NPF would have taken place without roll-induced NPF, such as the case study in Figure 4 ~~(see cases in Figure 5)~~.

4 Conclusions

We studied what is the effect of roll vortices on atmospheric NPF in the BL by analyzing airborne and ground-based measurements done over a rural boreal forest in southern Finland. We found that roll-induced NPF can considerably enhance the production of new aerosol particles over a boreal forest and these particles can grow to larger, potentially CCN, sizes, similar to particles produced by regional NPF. Roll-induced NPF seems to occur in only some of the roll vortices, which is likely related to variability in the rolls. In order to fully understand roll-induced NPF, better measurement and analysis methods need to be developed. For example measuring the fluxes of sub-10 nm particles and doing airborne flux measurements. More measurements with the turbulence probe on board need to be performed. It would also be interesting to study the cluster composition during roll-induced NPF.

~~The processes that lead to roll-induced NPF are conceptualized in Figure 10. Roll vortices strongly enhance mass transfer at the atmosphere-biosphere interface (Zilitinkevich et al., 2006). The narrow updrafts collect and efficiently deliver low-volatile gases and clusters from the surface to the upper parts of the BL where nucleation is more favorable due to lower temperatures and mixing over the inversion (Buzorius et al., 2001; Easter and Peters, 1994; Nilsson et al., 2001; Nilsson and Kulmala, 1998). The freshly-formed particles are then transported down by the downdrafts. We found that roll-induced NPF can considerably enhance the production of new aerosol particles over a boreal forest and these particles can grow to larger, potentially CCN, sizes, similar to particles produced by regional NPF. Roll-induced NPF seems to occur in only some of the roll vortices, which is likely related to variability in the rolls.~~

NPF is a ubiquitous phenomenon in the global atmosphere (Kerminen et al., 2018; Kulmala et al., 2004), likewise roll vortices are a common feature in the planetary BL around the world (Atkinson and Wu Zhang, 1996; Etling and Brown, 1993; Young et al., 2002). Therefore, roll-induced NPF is expected to take place in several other environments around the world as well. Hence, unstable stratification and the formation of roll vortices needs to be taken into account in order to understand the overall role of atmospheric NPF in particle number and CCN budgets.

Author contribution: JL, KL, RV, AM, SBM, HEM and JK carried out the airborne measurements. ML processed and interpreted the weather radar data. MB, SZ and HJ helped with the analysis of meteorological data. JL prepared the manuscript with contributions from all co-authors.

Acknowledgements: This project has received funding from the ERC advanced grant No. 742206, the European Union's Horizon 2020 research and innovation program under grant agreement No. 654109, the Academy of Finland Center of Excellence project No. 272041 and the European Commission under the Framework Programme 7 (FP7-ENV-2010-265148). S. Zilitinkevich acknowledges support from the Academy of Finland projects ABBA No. 280700 (2014-2017) and ClimEco No. 314 798/799 (2018-2020); and Russian Science Foundation project No. 15-17-20009 (2015-2018). We appreciate the efforts that the Zeppelin NT pilots and ground crews made to this work. We acknowledge Dr. T. F. Mentel and Dr. F. Rohrer from Forschungszentrum Jülich, Germany. We thank Erkki Järvinen and the pilots at Airspark Oy for operating the research airplane. We acknowledge the use of imagery from the NASA Worldview application (https://worldview.earthdata.nasa.gov/) operated by the NASA/Goddard Space Flight Center Earth Science Data and Information System (ESDIS) project.

References

Aalto, P., Hämeri, K., Becker, E., Weber, R., Salm, J., Mäkelä, J. M., Hoell, C., O'Dowd, C. D., Hansson, H.-C., Väkevä, M., Koponen, I. K., Buzorius, G. and Kulmala, M.: Physical characterization of aerosol particles during nucleation events, Tellus B, 53(4), 344–358, doi:10.3402/tellusb.v53i4.17127, 2001.

Atkinson, B. W. and Wu Zhang, J.: Mesoscale shallow convection in the atmosphere, Rev. Geophys., 34(4), 403–431, doi:10.1029/96RG02623, 1996.

Boucher, O., Randall, D., Artaxo, P., Bretherton, C., Feingold, G., Forster, P., Kerminen, V.-M., Kondo, Y., Liao, H., Lohmann, U., Rasch, P., Satheesh, S. K., Sherwood, S., Stevens, B. and Zhang, X. Y.: Clouds and Aerosols, in Climate Change 2013: The Physical Science Basis. Contribution of Working Group I to the Fifth Assessment Report of the Intergovernmental Panel on Climate Change, edited by T. F. Stocker, D. Qin, G.-K. Plattner, M. Tignor, S. K. Allen, J. Boschung, A. Nauels, Y. Xia, V. Bex, and P. M. Midgley, pp. 571–658, Cambridge University Press, Cambridge, United Kingdom and New York, NY, USA. [online] Available from: www.climatechange2013.org, 2013.

Brooks, I. M. and Rogers, D. P.: Aircraft Observations of Boundary Layer Rolls off the Coast of California, J. Atmospheric Sci., 54(14), 1834–1849, doi:10.1175/1520-0469(1997)054<1834:AOOBLR>2.0.CO;2, 1997.

Buzorius, G., Rannik, Ü., Mäkelä, J. M., Keronen, P., Vesala, T. and Kulmala, M.: Vertical aerosol fluxes measured by the eddy covariance method and deposition of nucleation mode particles above a Scots pine forest in southern Finland, J. Geophys. Res. Atmospheres, 105(D15), 19905–19916, doi:10.1029/2000JD900108, 2000.

Buzorius, G., Rannik, Ü., Nilsson, D. and Kulmala, M.: Vertical fluxes and micrometeorology during aerosol particle formation events, Tellus B, 53(4), 394–405, doi:10.1034/j.1600-0889.2001.530406.x, 2001.

Crumeyrolle, S., Manninen, H. E., Sellegri, K., Roberts, G., Gomes, L., Kulmala, M., Weigel, R., Laj, P. and Schwarzenboeck, A.: New particle formation events measured on board the ATR-42 aircraft during the EUCAARI campaign, Atmospheric Chem. Phys., 10(14), 6721–6735, doi:10.5194/acp-10-6721-2010, 2010.

Dada, L., Paasonen, P., Nieminen, T., Buenrostro Mazon, S., Kontkanen, J., Peräkylä, O., Lehtipalo, K., Hussein, T., Petäjä, T., Kerminen, V.-M., Bäck, J. and Kulmala, M.: Long-term analysis of clear-sky new particle formation events and nonevents in Hyytiälä, Atmos Chem Phys, 17(10), 6227–6241, doi:10.5194/acp-17-6227-2017, 2017.

Dunne, E. M., Gordon, H., Kürten, A., Almeida, J., Duplissy, J., Williamson, C., Ortega, I. K., Pringle, K. J., Adamov, A., Baltensperger, U., Barmet, P., Benduhn, F., Bianchi, F., Breitenlechner, M., Clarke, A., Curtius, J., Dommen, J., Donahue, N. M., Ehrhart, S., Flagan, R. C., Franchin, A., Guida, R., Hakala, J., Hansel, A., Heinritzi, M., Jokinen, T., Kangasluoma, J., Kirkby, J., Kulmala, M., Kupc, A., Lawler, M. J., Lehtipalo, K., Makhmutov, V., Mann, G., Mathot, S., Merikanto, J., Miettinen, P., Nenes, A., Onnela, A., Rap, A., Reddington, C. L. S., Riccobono, F., Richards, N. A. D., Rissanen, M. P., Rondo, L., Sarnela, N., Schobesberger, S., Sengupta, K., Simon, M., Sipilä, M., Smith, J. N., Stozkhov, Y., Tomé, A., Tröstl, J., Wagner, P. E., Wimmer, D., Winkler, P. M., Worsnop, D. R. and Carslaw, K. S.: Global atmospheric particle formation from CERN CLOUD measurements, Science, 354(6316), 1119–1124, doi:10.1126/science.aaf2649, 2016.

Easter, R. C. and Peters, L. K.: Binary homogeneous nucleation: temperature and relative humidity fluctuations, nonlinearity, and aspects of new particle production in the atmosphere, J. Appl. Meteorol., 33(7), 775–784, doi:10.1175/1520-0450(1994)033<0775:BHNTAR>2.0.CO;2, 1994.

Ehn, M., Thornton, J. A., Kleist, E., Sipilä, M., Junninen, H., Pullinen, I., Springer, M., Rubach, F., Tillmann, R., Lee, B., Lopez-Hilfiker, F., Andres, S., Acir, I.-H., Rissanen, M., Jokinen, T., Schobesberger, S., Kangasluoma, J., Kontkanen, J., Nieminen, T., Kurtén, T., Nielsen, L. B., Jørgensen, S., Kjaergaard, H. G., Canagaratna, M., Maso, M. D., Berndt, T., Petäjä, T., Wahner, A., Kerminen, V.-M., Kulmala, M., Worsnop, D. R., Wildt, J. and Mentel, T. F.: A large source of low-volatility secondary organic aerosol, Nature, 506(7489), 476–479, doi:10.1038/nature13032, 2014.

Etling, D. and Brown, R. A.: Roll vortices in the planetary boundary layer: A review, Bound.-Layer Meteorol., 65(3), 215–248, doi:10.1007/BF00705527, 1993.

Gordon, H., Kirkby, J., Baltensperger, U., Bianchi, F., Breitenlechner, M., Curtius, J., Dias, A., Dommen, J., Donahue, N. M., Dunne, E. M., Duplissy, J., Ehrhart, S., Flagan, R. C., Frege, C., Fuchs, C., Hansel, A., Hoyle, C. R., Kulmala, M., Kürten, A., Lehtipalo, K., Makhmutov, V., Molteni, U., Rissanen, M. P., Stozkhov, Y., Tröstl, J., Tsagkogeorgas, G., Wagner, R., Williamson, C., Wimmer, D., Winkler, P. M., Yan, C. and Carslaw, K. S.: Causes and importance of new particle formation in

the present-day and preindustrial atmospheres, J. Geophys. Res. Atmospheres, 122(16), 8739–8760, doi:10.1002/2017JD026844, 2017.

Gormley, P. G. and Kennedy, M.: Diffusion from a Stream Flowing through a Cylindrical Tube, Proc. R. Ir. Acad. Sect. Math. Phys. Sci., 52, 163–169, 1948.

Gryspeerdt, E., Stier, P. and Partridge, D. G.: Satellite observations of cloud regime development: the role of aerosol processes, Atmospheric Chem. Phys., 14(3), 1141–1158, doi:https://doi.org/10.5194/acp-14-1141-2014, 2014.

Hamed, A., Joutsensaari, J., Mikkonen, S., Sogacheva, L., Dal Maso, M., Kulmala, M., Cavalli, F., Fuzzi, S., Facchini, M. C., Decesari, S., Mircea, M., Lehtinen, K. E. J. and Laaksonen, A.: Nucleation and growth of new particles in Po Valley, Italy, Atmos Chem Phys, 7(2), 355–376, doi:10.5194/acp-7-355-2007, 2007.

Hari, P. and Kulmala, M.: Station for measuring ecosystem-atmosphere relations (SMEAR II), Boreal Environ. Res., 10(5), 315–322, 2005.

Kerminen, V.-M., Paramonov, M., Anttila, T., Riipinen, I., Fountoukis, C., Korhonen, H., Asmi, E., Laakso, L., Lihavainen, H., Swietlicki, E., Svenningsson, B., Asmi, A., Pandis, S. N., Kulmala, M. and Petäjä, T.: Cloud condensation nuclei production associated with atmospheric nucleation: a synthesis based on existing literature and new results, Atmospheric Chem. Phys., 12(24), 12037–12059, doi:https://doi.org/10.5194/acp-12-12037-2012, 2012.

Kerminen, V.-M., Chen, X., Vakkari, V., Petäjä, T., Kulmala, M. and Bianchi, F.: Atmospheric new particle formation and growth: review of field observations, Environ. Res. Lett., 13(10), 103003, doi:10.1088/1748-9326/aadf3c, 2018.

Kulmala, M., Vehkamäki, H., Petäjä, T., Dal Maso, M., Lauri, A., Kerminen, V.-M., Birmili, W. and McMurry, P. H.: Formation and growth rates of ultrafine atmospheric particles: a review of observations, J. Aerosol Sci., 35(2), 143–176, doi:10.1016/j.jaerosci.2003.10.003, 2004.

Kulmala, M., Petäjä, T., Nieminen, T., Sipilä, M., Manninen, H. E., Lehtipalo, K., Dal Maso, M., Aalto, P. P., Junninen, H., Paasonen, P., Riipinen, I., Lehtinen, K. E. J., Laaksonen, A. and Kerminen, V.-M.: Measurement of the nucleation of atmospheric aerosol particles, Nat. Protoc., 7(9), 1651–1667, doi:10.1038/nprot.2012.091, 2012.

Leino, K., Lampilahti, J., Poutanen, P., Väänänen, R., Manninen, A., Buenrostro Mazon, S., Dada, L., Franck, A., Wimmer, D., Aalto, P. P., Ahonen, L. R., Enroth, J., Kangasluoma, J., Keronen, P., Korhonen, F., Laakso, H., Matilainen, T., Siivola, E., Manninen, H. E., Lehtipalo, K., Kerminen, V.-M., Petäjä, T. and Kulmala, M.: Vertical profiles of sub-3 nm particles over the boreal forest, Atmospheric Chem. Phys., 19(6), 4127–4138, doi:https://doi.org/10.5194/acp-19-4127-2019, 2019.

Manninen, H. E., Petäjä, T., Asmi, E., Riipinen, N., Nieminen, T., Mikkilä, J., Horrak, U., Mirme, A., Mirme, S., Laakso, L., Kerminen, V.-M. and Kulmala, M.: Long-term field measurements of charged and neutral clusters using Neutral cluster and Air Ion Spectrometer (NAIS), Boreal Environ. Res., 14(4), 591–605, 2009.

Mirme, S. and Mirme, A.: The mathematical principles and design of the NAIS – a spectrometer for the measurement of cluster ion and nanometer aerosol size distributions, Atmospheric Meas. Tech., 6(4), 1061–1071, doi:10.5194/amt-6-1061-2013, 2013.

Mirme, S., Mirme, A., Minikin, A., Petzold, A., Hõrrak, U., Kerminen, V.-M. and Kulmala, M.: Atmospheric sub-3 nm particles at high altitudes, Atmospheric Chem. Phys., 10(2), 437–451, doi:10.5194/acp-10-437-2010, 2010.

Miura, Y.: Aspect ratios of longitudinal rolls and convection cells observed during cold air outbreaks, J. Atmospheric Sci., 43(1), 26–39, doi:10.1175/1520-0469(1986)043<0026:AROLRA>2.0.CO;2, 1986.

Nieminen, T., Asmi, A., Dal Maso, M., Aalto, P. P., Keronen, P., Petäjä, T., Kulmala, M. and Kerminen, V.-M.: Trends in atmospheric new-particle formation: 16 years of observations in a boreal-forest environment, Boreal Environ. Res., 19, 191–214, 2014.

Nilsson, E. D. and Kulmala, M.: The potential for atmospheric mixing processes to enhance the binary nucleation rate, J. Geophys. Res. Atmospheres, 103(D1), 1381–1389, doi:10.1029/97JD02629, 1998.

Nilsson, E. D., Rannik, Ü., Kulmala, M., Buzorius, G. and O'dowd, C. D.: Effects of continental boundary layer evolution, convection, turbulence and entrainment, on aerosol formation, Tellus B, 53(4), 441–461, doi:10.1034/j.1600-0889.2001.530409.x, 2001.

O'Dowd, C. D., Yoon, Y. J., Junkermann, W., Aalto, P., Kulmala, M., Lihavainen, H. and Viisanen, Y.: Airborne measurements of nucleation mode particles II: boreal forest nucleation events, Atmospheric Chem. Phys., 9(3), 937–944, doi:10.5194/acp-9-937-2009, 2009.

Platis, A., Altstädter, B., Wehner, B., Wildmann, N., Lampert, A., Hermann, M., Birmili, W. and Bange, J.: An Observational Case Study on the Influence of Atmospheric Boundary-Layer Dynamics on New Particle Formation, Bound.-Layer Meteorol., 158(1), 67–92, doi:10.1007/s10546-015-0084-y, 2015.

Rosenfeld, D., Andreae, M. O., Asmi, A., Chin, M., Leeuw, G. de, Donovan, D. P., Kahn, R., Kinne, S., Kivekäs, N., Kulmala, M., Lau, W., Schmidt, K. S., Suni, T., Wagner, T., Wild, M. and Quaas, J.: Global observations of aerosol-cloud-precipitation-climate interactions, Rev. Geophys., 52(4), 750–808, doi:10.1002/2013RG000441, 2014.

Schobesberger, S., Väänänen, R., Leino, K., Virkkula, A., Backman, J., Pohja, T., Siivola, E., Franchin, A., Mikkilä, J., Paramonov, M., Aalto, P. P., Krejci, R., Petäjä, T. and Kulmala, M.: Airborne measurements over the boreal forest of southern Finland during new particle formation events in 2009 and 2010, Boreal Environ. Res., 18(2), 145–164, 2013.

Seidel, D. J., Ao, C. O. and Li, K.: Estimating climatological planetary boundary layer heights from radiosonde observations: Comparison of methods and uncertainty analysis, J. Geophys. Res. Atmospheres, 115(D16), D16113, doi:10.1029/2009JD013680, 2010.

Siebert, H., Stratmann, F. and Wehner, B.: First observations of increased ultrafine particle number concentrations near the inversion of a continental planetary boundary layer and its relation to ground-based measurements, Geophys. Res. Lett., 31(9), doi:10.1029/2003GL019086, 2004.

Smedman, A.-S.: Occurrence of roll circulations in a shallow boundary layer, Bound.-Layer Meteorol., 57(4), 343–358, doi:10.1007/BF00120053, 1991.

Väänänen, R., Krejci, R., Manninen, H. E., Manninen, A., Lampilahti, J., Buenrostro Mazon, S., Nieminen, T., Yli-Juuti, T., Kontkanen, J., Asmi, A., Aalto, P. P., Keronen, P., Pohja, T., O'Connor, E., Kerminen, V.-M., Petäjä, T. and Kulmala, M.: Vertical and horizontal variation of aerosol number size distribution in the boreal environment, Atmospheric Chem. Phys. Discuss., Manuscript in review, doi:10.5194/acp-2016-556, 2016.

Vandemark, D., Mourad, P. D., Bailey, S. A., Crawford, T. L., Vogel, C. A., Sun, J. and Chapron, B.: Measured changes in ocean surface roughness due to atmospheric boundary layer rolls, J. Geophys. Res. Oceans, 106(C3), 4639–4654, doi:10.1029/1999JC000051, 2001.

Vanhanen, J., Mikkilä, J., Lehtipalo, K., Sipilä, M., Manninen, H. E., Siivola, E., Petäjä, T. and Kulmala, M.: Particle size magnifier for nano-CN detection, Aerosol Sci. Technol., 45(4), 533–542, doi:10.1080/02786826.2010.547889, 2011.

Wainwright, C. E., Stepanian, P. M., Reynolds, D. R. and Reynolds, A. M.: The movement of small insects in the convective boundary layer: linking patterns to processes, Sci. Rep., 7(1), 5438, doi:10.1038/s41598-017-04503-0, 2017.

Wehner, B., Siebert, H., Ansmann, A., Ditas, F., Seifert, P., Stratmann, F., Wiedensohler, A., Apituley, A., Shaw, R. A., Manninen, H. E. and Kulmala, M.: Observations of turbulence-induced new particle formation in the residual layer, Atmospheric Chem. Phys., 10(9), 4319–4330, doi:10.5194/acp-10-4319-2010, 2010.

Wilson, J. W., Weckwerth, T. M., Vivekanandan, J., Wakimoto, R. M. and Russell, R. W.: Boundary layer clear-air radar echoes: Origin of echoes and accuracy of derived winds, J. Atmospheric Ocean. Technol., 11(5), 1184–1206, doi:10.1175/1520-0426(1994)011<1184:BLCARE>2.0.CO;2, 1994.

Young, G. S., Kristovich, D. A., Hjelmfelt, M. R. and Foster, R. C.: Rolls, streets, waves and more: A review of quasi-two-dimensional structures in the atmospheric boundary layer, Bull. Am. Meteorol. Soc., 83(7), ES54–ES69, 2002.

Zilitinkevich, S. S., Hunt, J. C. R., Esau, I. N., Grachev, A. A., Lalas, D. P., Akylas, E., Tombrou, M., Fairall, C. W., Fernando, H. J. S., Baklanov, A. A. and Joffre, S. M.: The influence of large convective eddies on the surface-layer turbulence, Q. J. R. Meteorol. Soc., 132(618), 1426–1456, doi:10.1256/qj.05.79, 2006.

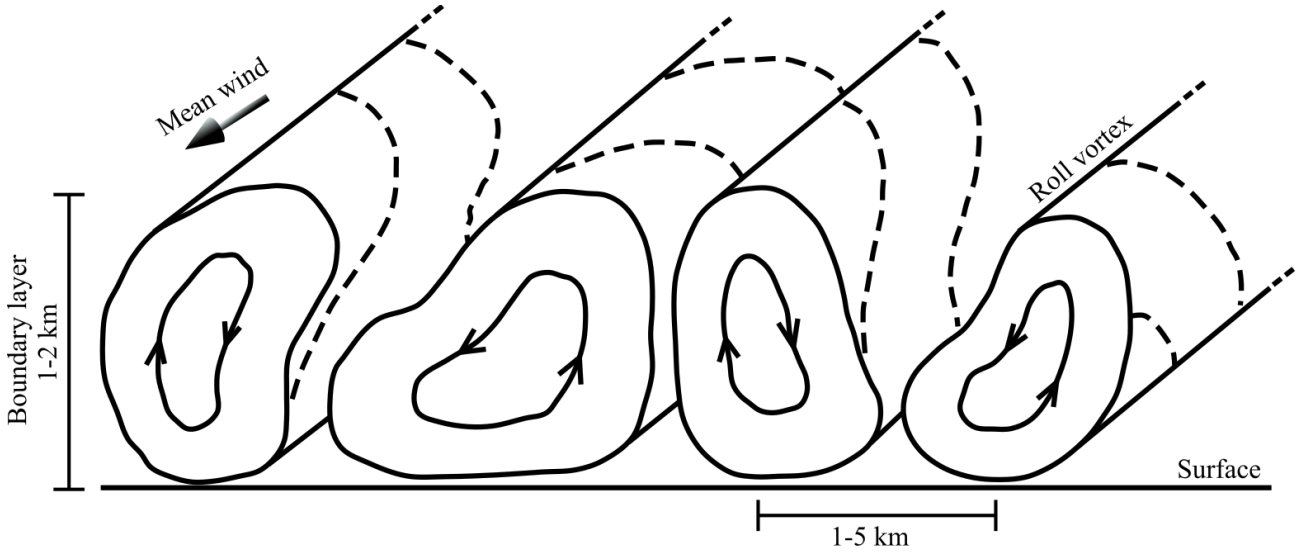

560

Figure 1: A schematic drawing of roll vortices in the boundary layer.

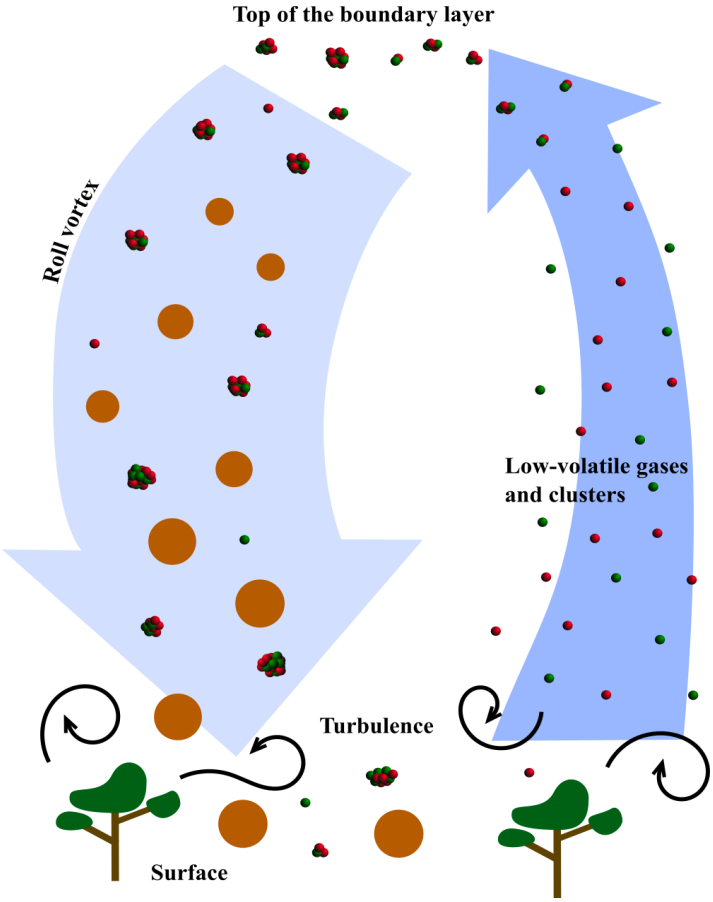

Figure 2: A schematic illustration of roll-induced NPF when viewed along a roll.

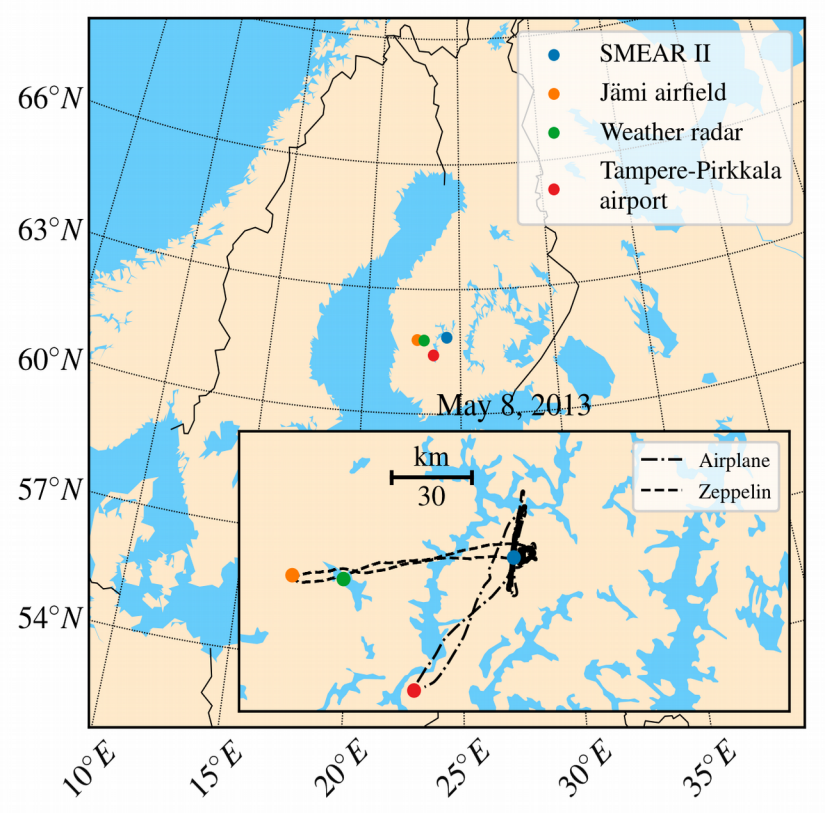

Figure 31: The locations of the Tampere-Pirkkala airport (ICAO: EFTP), Jämi airfield (ICAO: EFJM), Ikaalinen weather radar and SMEAR II station marked on a map. As an example, the aircraft measurement tracks on May 8, 2013 are included.

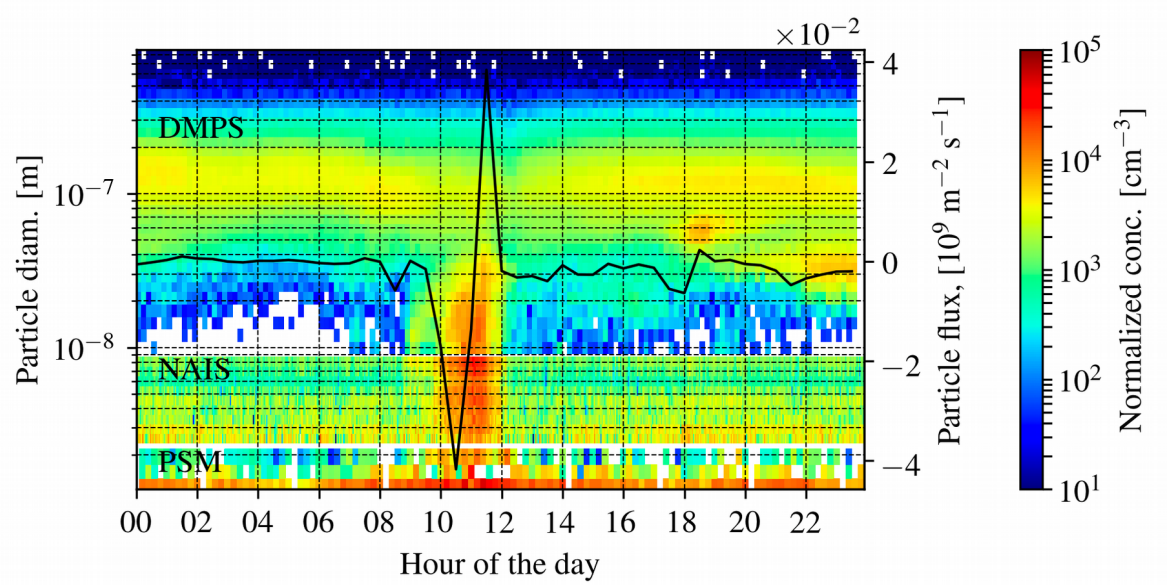

Figure 42: The particle number-size distribution in the range 1-1000 nm (composite of PSM, NAIS and DMPS data, see the Methods for instrument details) measured at the SMEAR II station on August 21, 2015. The black line is the vertical flux of >10 nm particles measured above the forest canopy (23 m height, negative sign means downward flux~~). Freshly formed clusters and aerosol particles were observed between 10:00 and 12:00. The particle number concentration for >1.5 nm particles increased from 2000 cm^{-3} in the background up to 18500 cm^{-3}. Simultaneous airborne measurements over the SMEAR II station revealed that the number concentration maxima were linked to specific adjacent roll vortices (Figure 3~~).

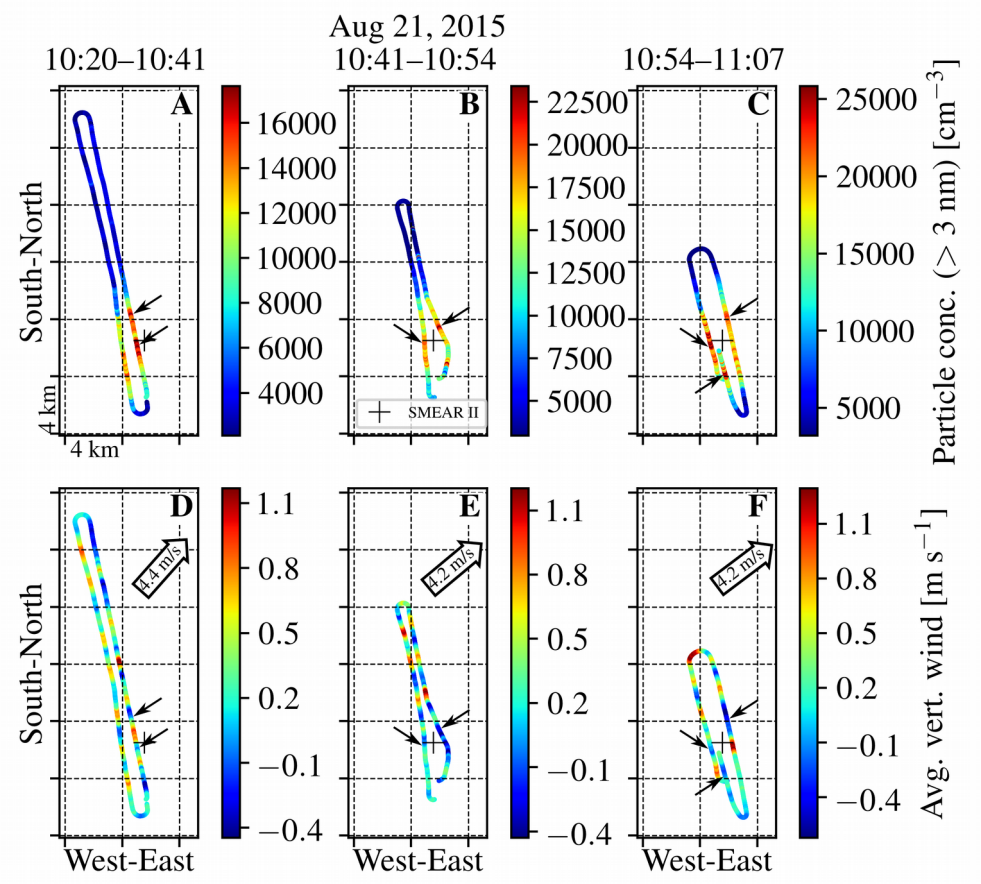

Figure 5: In panels A-C the sections of the measurement aiplane's flight track are colored by >3 nm particle number concentration. The grids have a 4-by-4 km spacing, the plus sign marks the position of the SMEAR II station and the time intervals for the flight track sections are displayed on top of the panels. In panels D-F the same flight tracks are colored by vertical wind speed smoothed using 30-sec moving average. The positive sign refers to updraft and the negative sign to downdraft. The large arrows show the mean wind speed and direction measured on board the airplane. The flight tracks were flown inside the convective BL between 120 m and 620 m above ground. The small arrows show that the maxima in the particle number concentration were located in the roll downdrafts.

Figure 3: In panels A-C the sections of the measurement aiplane's flight track are colored by >3 nm particle number concentration. The grids have a 4-by-4 km spacing, the plus sign marks the position of the SMEAR II station and the time intervals for the flight track sections are displayed on top of the panels. In panels D-F the same flight tracks are colored by vertical wind speed smoothed using 30-sec moving average. The positive sign refers to updraft and the negative sign to downdraft. The large arrows show the mean wind speed and direction measured on board the airplane. The flight tracks were flown inside the convective BL between 120 m and 620 m above ground. The roll-induced NPF was observed in the southern part of the flight track directly on top of the SMEAR II station. The vertical wind speed measurements on board the airplane revealed the presence of rolls as regularly alternating up- and downdrafts that were aligned with the mean wind, over the flight path. The small arrows show that the maxima in the particle number concentration were located in the roll downdrafts.

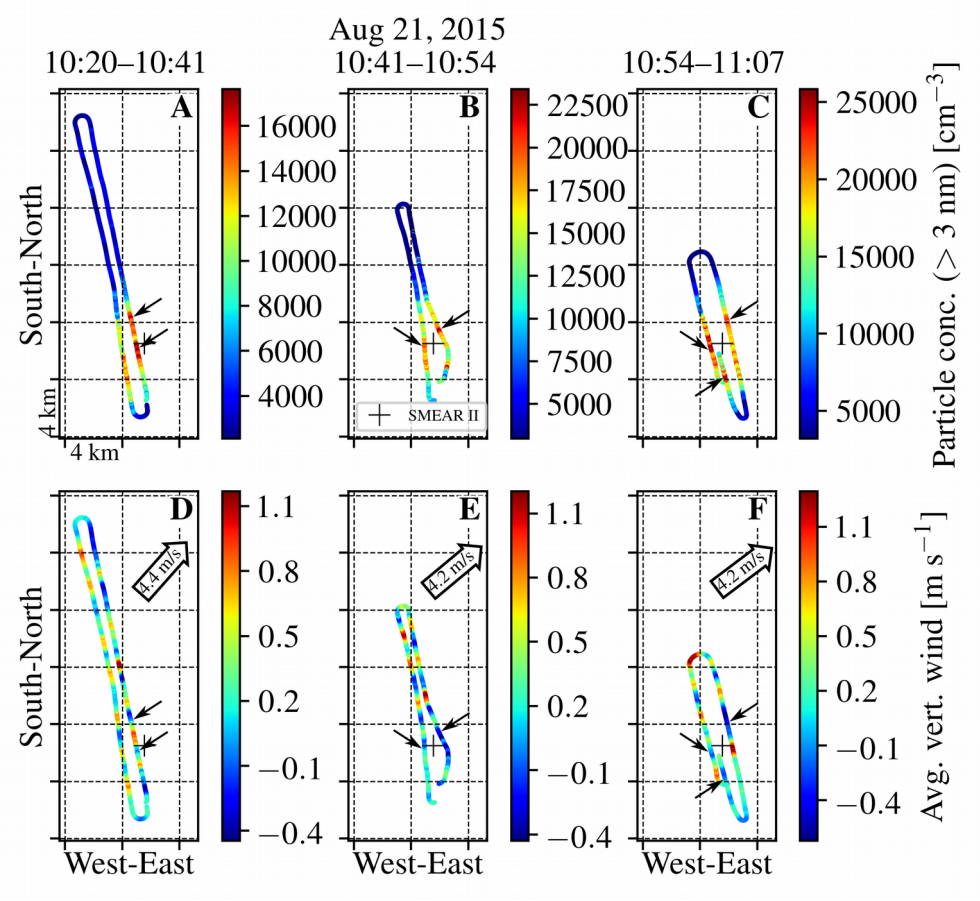

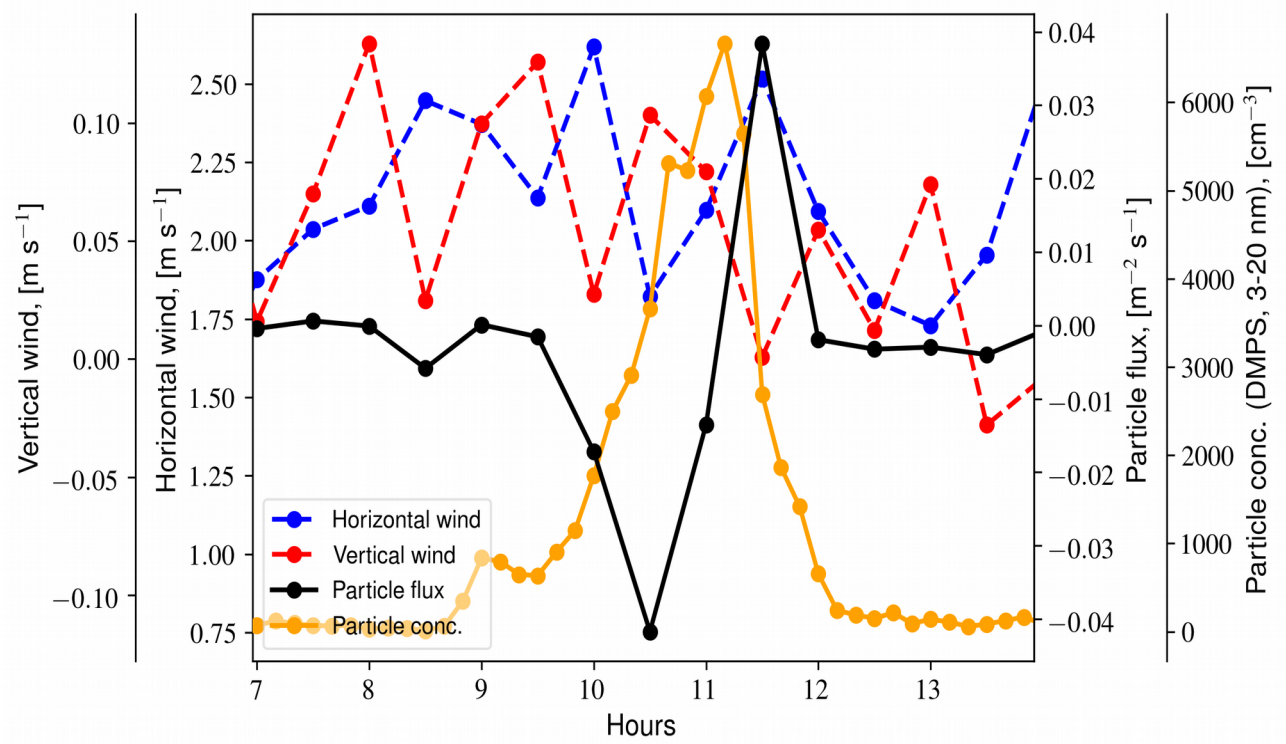

595 **Figure 6:** Time series of the vertical wind (33.6 m above ground), horizontal wind (33.6 m above ground), vertical flux of >10 nm particles (23 m above ground) and number concentration of 3-20 nm particles inside the canopy (8 m above ground) on Aug 21, 2015.

Figure 4: Time series of the vertical wind, horizontal wind, vertical flux of >10 nm particles (averaged to 30 min, measured at 23 m above ground or 1-2 m above canopy) and number concentration of >3 nm particles inside the canopy on Aug 21, 2015. The periodic anti-correlation between the wind components is a clear indication of roll vortices drifting over the measurement location perpendicular to the mean wind direction. This is due to a slight difference between the direction of the mean wind and the roll axis. During a sunny August day with moderate wind, turbulence dominates vertical transport close to the canopy, so the variations in particle number concentration and vertical particle flux close to the canopy are decoupled from the roll circulation. When the roll-induced NPF first moves over the field site the number concentration above the turbulent layer increases and the particles start to mix downwards. Inside the turbulent layer the particle flux becomes negative and the number concentration starts to increase. As more and more particles are mixed downwards, the number concentration increases inside the turbulent layer while the particle flux becomes less negative. As the roll-induced NPF moves away, the vertical particle flux can become positive if the number concentration below the flux measurement is higher than above.

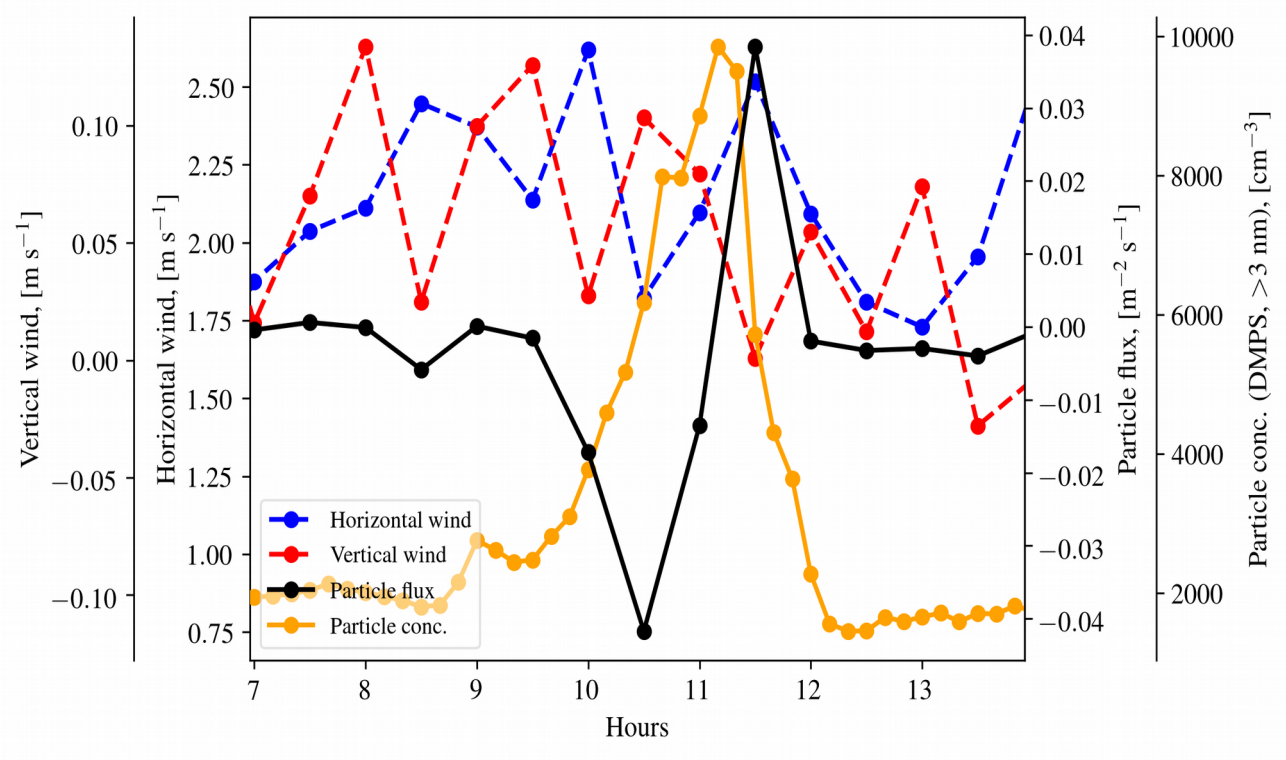

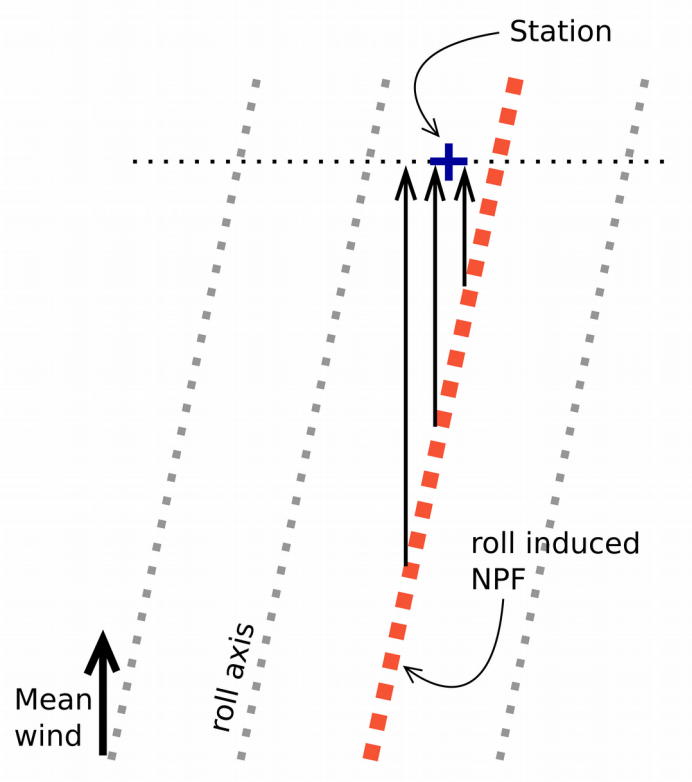

Figure 7: Schematic diagram illustrating how a difference in the direction of the mean wind and the roll axis causes the rolls (and the roll-induced NPF) to move over a stationary point perpendicular to the mean wind direction.

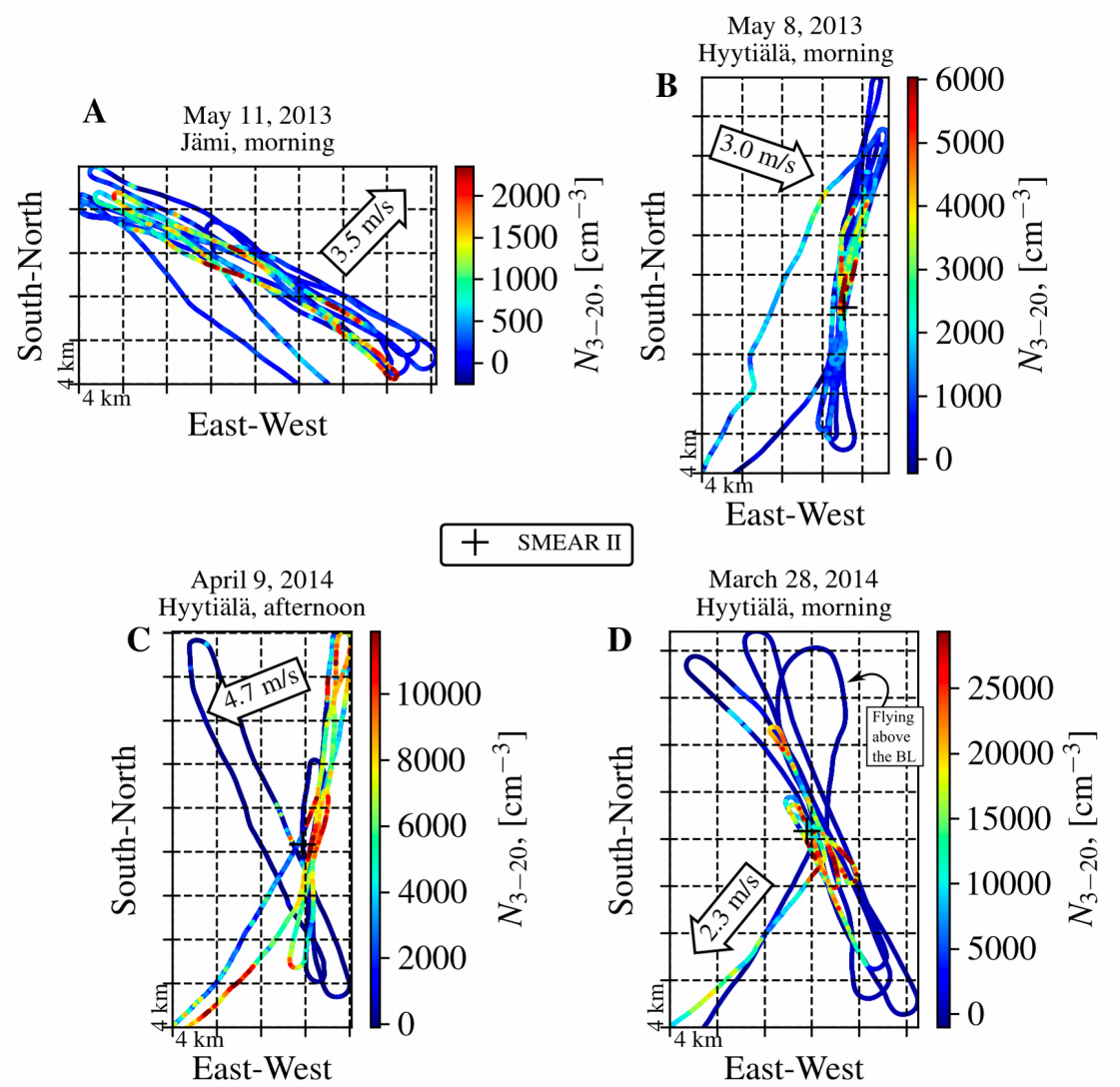

Figure 85: Panels A-D show the research airplane's flight tracks colored by particle number concentration in the 3-20 nm diameter range on four different measurement flights. The higher particle number concentrations are displayed on top in order to make the roll-induced NPF more clearly visible. ~~The locations of roll-induced NPF were observed as narrow areas of increased particle number concentration perpendicular to the mean wind direction that persisted over multiple successive overpasses. They were not seen when the airplane was flying above the convective BL. Above the BL the particle number concentration was about an order of magnitude lower.~~ The arrows show the mean wind direction and speed from the SMEAR II mast.

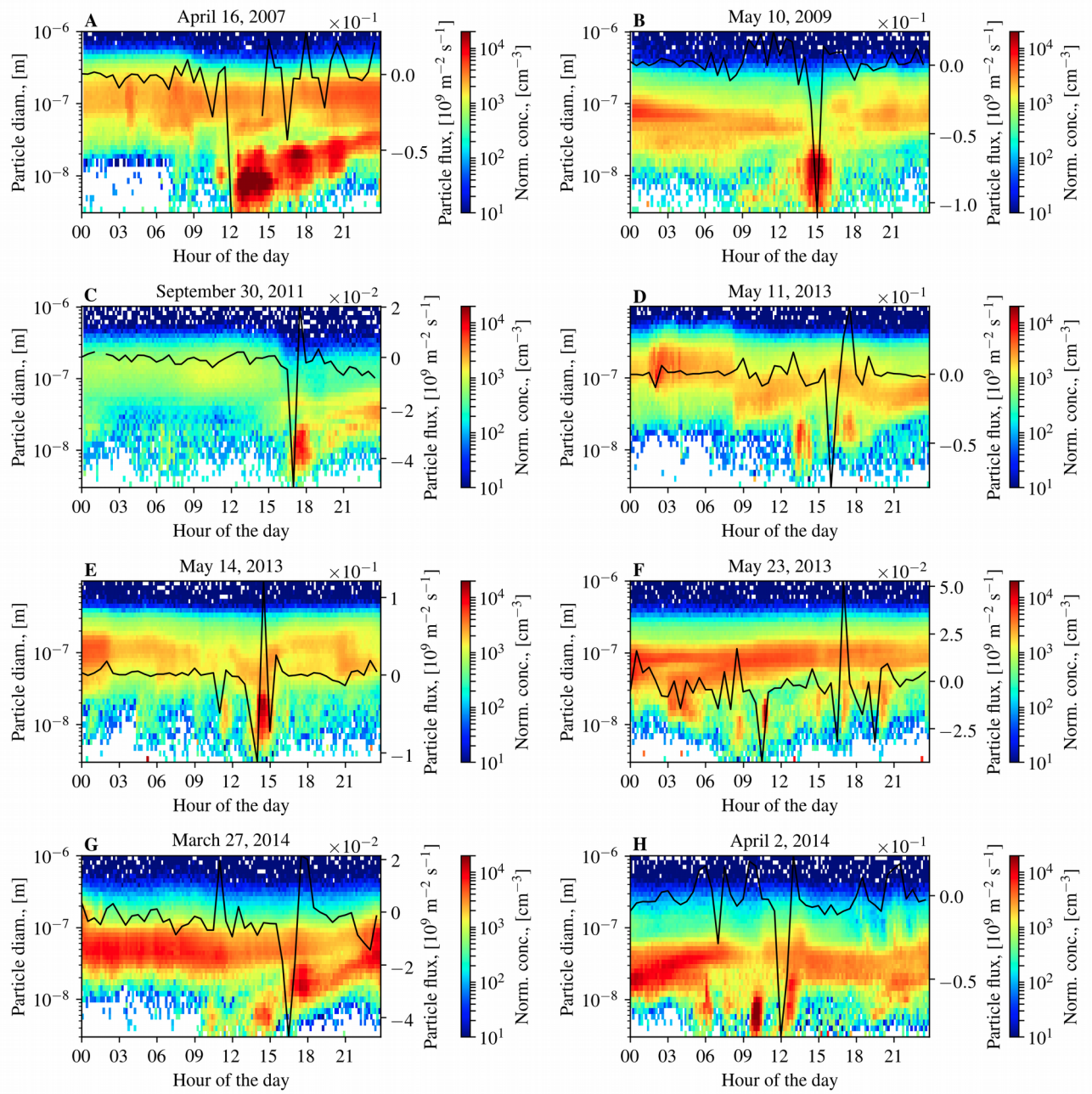

Figure 96: The panels A-H show 3-1000 nm particle number-size distribution measured at the SMEAR II station by the DMPS during some of the days when there was roll-induced NPF. In addition the black line shows the vertical flux of >10 nm particles measured at 23 m height. ~~The roll-induced NPF was marked by momentary increase in sub-20 nm particles, coupled with a relatively large fluctuation in vertical particle flux compared to background. If not enough of the particles were above 10 nm, then no clear fluctuation in the particle flux can be seen.~~

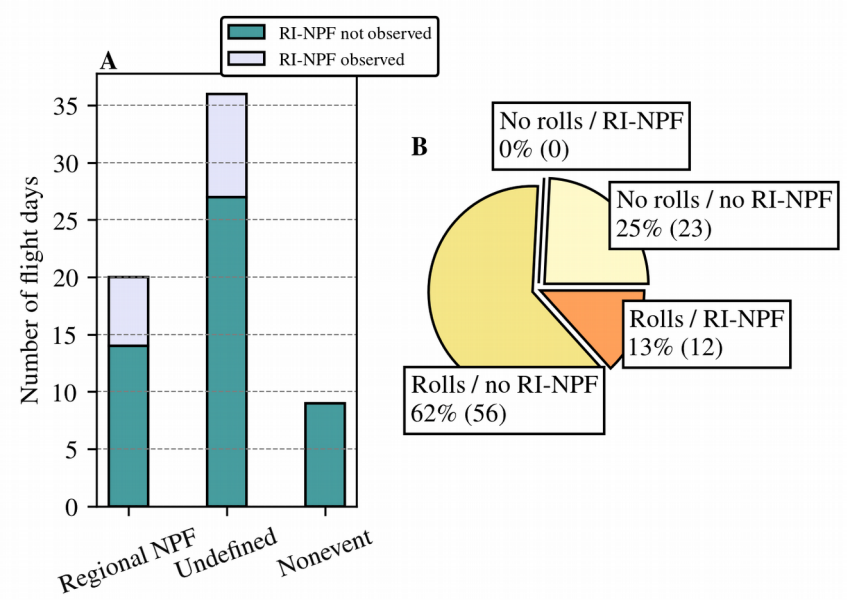

Figure 10: Panel A shows how the roll-induced NPF (RI-NPF) observations distribute into different NPF event classes on the flight days. Panel B shows the classification of each measurement flight into four different classes based on whether rolls and/or RI-NPF over the same area was observed or not. Note that the data in panel A consists of flight days while the data in panel B consists of individual flights (there could be more than one flight per day).

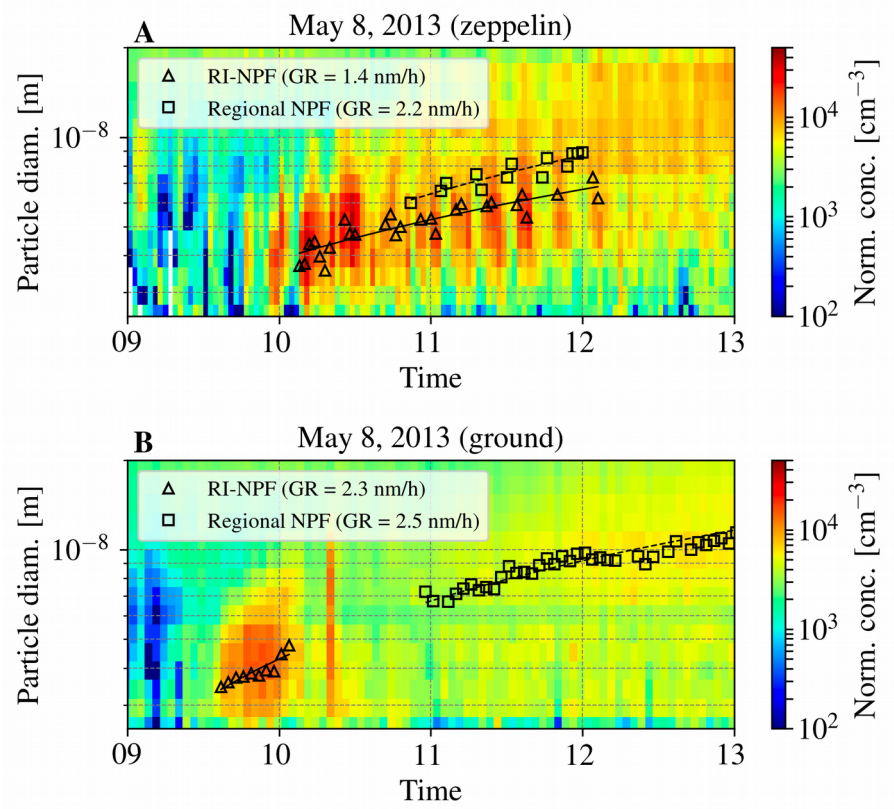

Figure 11: The particle number-size distribution (positive polarity) between 2.5-20 nm measured by the NAIS (A) on board the zeppelin and (B) at the field station on May 8, 2013. Between 10-12 the zeppelin consecutively flew through the roll-induced NPF (RI-NPF) event, leaving concentrated "stripes" on the particle number-size distribution. Between 9:30-10:00 the roll-induced NPF event moved over the field station. The black triangles and squares show the fitted mean mode diameters to the roll-induced and regional NPF event particles, respectively. Figure 8B shows simultaneous observations from the airplane. The roll-induced NPF event was moving over the measurement area from southwest to northeast. Weather radar observations showed that rolls were present over the measurement site and power spectra of the wind components from the station's mast showed that the rolls were moving over the site at the same rate (one roll in ~20 min), and in the same direction as the roll-induced NPF..

Figure 7: Panel A shows that roll-induced NPF (RI-NPF) was observed on 23% of the flight measurement days, 30% of the NPF event days and 22% of the days classified as undefined. Panel B shows the association between roll-induced NPF and roll observations from radar and satellite images. The data in panel A consists of flight days while the data in panel B consists of individual flights (note that there could be two flights per day, see Table 1). Rolls were always present during roll-induced NPF and according to Fisher's exact test this association was significant (p=0.03). The fact that rolls did not induce NPF every time means that other necessary factors for atmospheric NPF (e.g. photochemistry, sinks) were likely not satisfied.

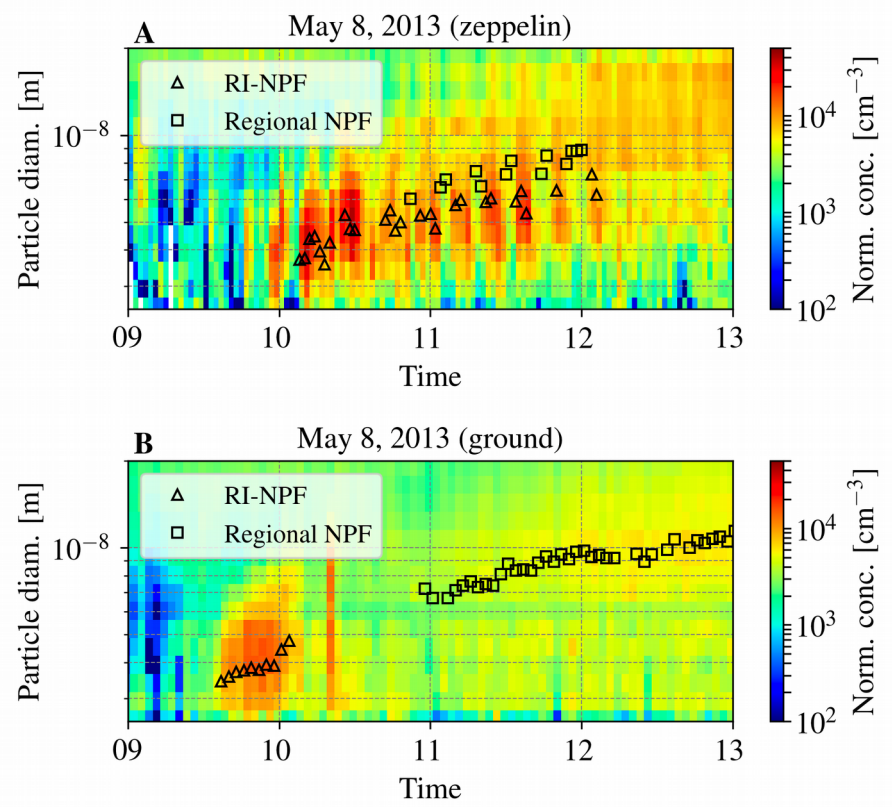

655 ~~**Figure 8:** The particle number-size distribution (positive polarity) between 2.5-20 nm measured by the NAIS (A) on board the zeppelin and (B) at the field station on May 8 2013. Between 10-12 the zeppelin consecutively flew through the roll-induced NPF (RI-NPF) event, leaving concentrated "stripes" on the particle number-size distribution. Between 9:30-10:00 the roll-induced NPF event moved over the field station. The black triangles and squares show the fitted mean mode diameters to the roll-induced and~~
660 ~~regional NPF event particles, respectively. Figure 5B shows simultaneous observations from the airplane, however there were no wind measurements on board. Weather radar observations showed that rolls were present over the measurement site and power spectra of the wind components from the station's mast showed that the rolls were moving over the site.~~

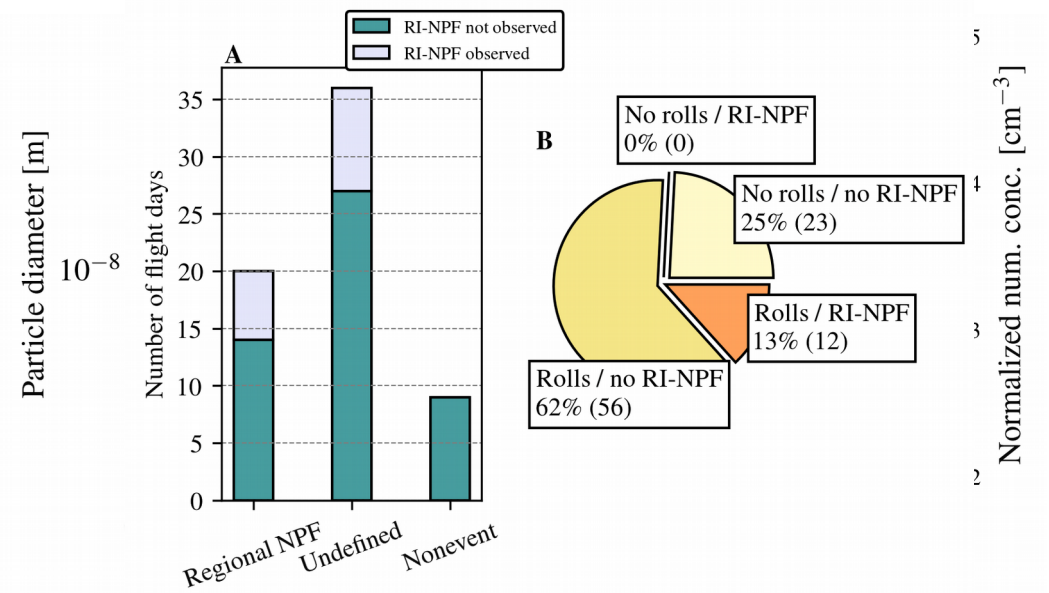

Figure 129: The above particle number-size distribution was constructed using the SMEAR II station's
665 NAIS data by taking the roll-induced NPF observations ~~presented in Table 3~~ (29 days and 46 different roll-induced NPF events) and distributing them along the time axis according to their geometric mean diameter while assuming a growth rate of 1.9 nm/h (median of the obtained GRs) and start of the NPF at t=0 hours. We used random sampling to estimate the median and the 25th~~h, which was calculated from days that showed~~

multiple subsequent roll-induced NPF events (13 days). The resulting number-size distribution was averaged to 1-hour bins and the variance in each bin was noted. We then used random sampling (1000 samples), also varying the GR, to estimate 25th, 50th and 75th percentile values for the formation rates of 3- and 10-nm-sized particles.

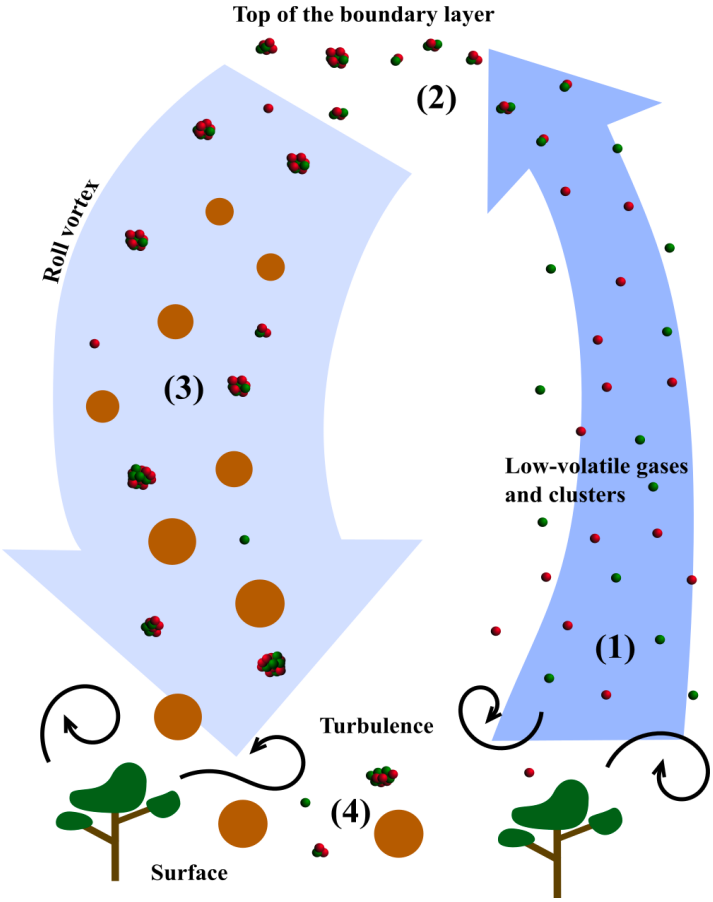

~~**Figure 10:** A schematic illustration of roll-induced NPF. The arrows depict the updraft and the downdraft zones of a single roll vortex, viewed along the roll. (1) in the boreal forest the vegetation is an important source of volatile organic compounds that can be oxidized into low-volatile organic vapors (Ehn et al., 2014). Due to higher wind speeds the shear-generation of turbulence close to the vegetation is stronger in rolls than in cellular type convection (Zilitinkevich et al., 2006). Therefore, roll updrafts are particularly efficient at transporting vapors and molecular clusters from the surface to the top of the BL. (2) on top of the BL decreased temperature, turbulence and mixing over the inversion layer can lead to a supersaturation of the vapors and activation of the clusters, leading to subsequent NPF (Easter and Peters, 1994; Nilsson and Kulmala, 1998). (3) the newly-formed particles grow in size in the weaker and wider downdraft and end up close to the surface where (4) they may be deposited on surfaces or continue growing while being transported in the air.~~

Table 1: Summary of airborne measurement campaigns from which data was utilized in this study. ~~Explanations:~~ PNSD = particle number-size distribution, INSD = ion number-size distribution, PNC = particle number concentration.

Time Place	Number of flight days	Measurement platform(s)	Instruments on board the aircrafts that were used in this study
May-Jun 2013 Hyytiälä, Finland	26	Zeppelin NT Cessna 172	Zeppelin NT • NAIS: 2-42 nm PNSD and 0.8-42 nm positive and negative INSD • Meteorological sensors: static pressure, temperature and relative humidity Cessna 172
Mar-Apr 2014 Hyytiälä, Finland	12	Cessna 172	
May-Jun 2014 Hyytiälä, Finland	5	Cessna 172	

Aug-Sept 2014, Hyytiälä, Finland	6	Cessna 172	
May-Jun 2015 Hyytiälä, Finland	7	Cessna 172	
Aug 2015 Hyytiälä, Finland	9	Cessna 172	• UCPC (TSI 3776 CPC): >3 nm PNC • SMPS: 10-400 nm PNSD • Li-Cor Li-840: CO2 and H2O vapor concentration • Meteorological sensors: static
~~Time Place~~	~~Number of flight days~~	~~Measurement platform(s)~~	~~Instruments on board the aircrafts that were used in this study~~
~~May-Jun 2013 Hyytiälä, Finland~~	~~26~~	~~Zeppelin NT Cessna 172~~	~~Zeppelin NT~~ ~~• NAIS: 2-42 nm PNSD and 0.8-42 nm positive and negative INSD~~ ~~• Meteorological sensors: static pressure, temperature and relative humidity~~ ~~Cessna 172~~ ~~• TSI 3776 CPC: >3 nm PNC~~ ~~• SMPS: 10-400 nm PNSD~~ ~~• Li-Cor Li-840: CO2 and H2O vapor concentration~~ ~~• Meteorological sensors: static pressure, temperature and relative humidity~~ ~~Cessna 172 (Aug 2015, last half of the campaign)~~ ~~• AIMMS-20: 3d wind vector~~
~~Mar-Apr 2014 Hyytiälä, Finland~~	~~12~~	~~Cessna 172~~	
~~May-Jun 2014 Hyytiälä, Finland~~	~~5~~	~~Cessna 172~~	
~~Aug-Sept 2014, Hyytiälä, Finland~~	~~6~~	~~Cessna 172~~	
~~May-Jun 2015 Hyytiälä, Finland~~	~~7~~	~~Cessna 172~~	
~~Aug 2015 Hyytiälä, Finland~~	~~9~~	~~Cessna 172~~	

Table 2. A summary of the flight campaign observations. Explanations: AM=morning flight, PM=afternoon flight, N=not observed, I=roll-induced NPF observed from the airplane, II=roll-induced NPF observed from the field station, R=roll vortices present over the measurement area, C=clear air (presence of rolls inconclusive), RE=regional NPF event observed, UD=undefined day, NE=nonevent day.

Flight	Roll-induced NPF	Rolls	NPF event class
20130506 AM	N	R	RE
20130506 PM	N	R	
20130507 AM	N	R	UD
20130507 PM	N	R	
20130508 AM	I/II	R	RE
20130508 PM	N	R	
20130511 AM	I/II	R	UD
20130511 PM	N	R	
20130514 AM*	II	R	UD
20130515 AM	N	R	RE
20130516 AM	I	R	RE
20130516 PM	I	R	
20130517 AM	N	R	NE
20130518 AM	N	N	UD
20130520 AM	N	R	UD
20130521 AM	N	R	UD
20130522 AM	I	R	UD
20130522 PM	N	N	
20130523 AM	I/II	R	UD
20130523 PM	N	N	
20130525 AM	I	R	UD
20130526 AM	N	R	UD
20130526 PM	I	R	
20130528 AM	N	R	NE

~~20130529 AM~~	~~N~~	~~R~~	~~UD~~
~~20130602 AM~~	~~N~~	~~R~~	~~UD~~
~~20130602 PM~~	~~N~~	~~R~~	
~~20130603 AM~~	~~N~~	~~R~~	~~UD~~
~~20130603 PM~~	~~N~~	~~N~~	
~~20130605 PM~~	~~N~~	~~N~~	~~UD~~
~~20130606 AM~~	~~N~~	~~R~~	~~UD~~
~~20130606 PM~~	~~N~~	~~N~~	
~~20130608 AM~~	~~N~~	~~N~~	~~UD~~
~~20130608 PM~~	~~N~~	~~N~~	
~~20130609 AM~~	~~N~~	~~R~~	~~UD~~
~~20130610 AM~~	~~N~~	~~R~~	~~UD~~
~~20130610 PM~~	~~N~~	~~N~~	
~~20130613 AM~~	~~N~~	~~R~~	~~UD~~
~~20130613 PM~~	~~N~~	~~R~~	
~~20130615 AM~~	~~N~~	~~R~~	~~RE~~
~~20140325 AM~~	~~N~~	~~C~~	~~RE~~
~~20140325 PM~~	~~N~~	~~C~~	
~~20140326 AM~~	~~N~~	~~C~~	~~RE~~
~~20140326 PM~~	~~N~~	~~C~~	
~~20140327 AM~~	~~N~~	~~C~~	~~RE~~
~~20140327 PM~~	~~I/II~~	~~C~~	
~~20140328 AM~~	~~I~~	~~C~~	~~RE~~
~~20140328 PM~~	~~N~~	~~C~~	
~~20140331 AM~~	~~N~~	~~C~~	~~RE~~
~~20140331 PM~~	~~N~~	~~C~~	
~~20140401 AM~~	~~N~~	~~N~~	~~RE~~
~~20140401 PM~~	~~N~~	~~N~~	
~~20140402 AM~~	~~I/II~~	~~R~~	~~UD~~
~~20140402 PM~~	~~N~~	~~R~~	

~~20140403 AM~~	~~N~~	~~N~~	~~RE~~
~~20140403 PM~~	~~N~~	~~N~~	
~~20140407 AM~~	~~N~~	~~N~~	~~UD~~
~~20140408 AM~~	~~I~~	~~C~~	~~RE~~
~~20140408 PM~~	~~N~~	~~C~~	
~~20140409 AM~~	~~I~~	~~C~~	~~RE~~
~~20140409 PM~~	~~I~~	~~C~~	
~~20140410 AM~~	~~N~~	~~C~~	~~RE~~
~~20140410 PM~~	~~N~~	~~C~~	
~~20140522 AM~~	~~N~~	~~R~~	~~UD~~
~~20140523 AM~~	~~N~~	~~N~~	~~UD~~
~~20140523 PM~~	~~N~~	~~R~~	
~~20140602 AM~~	~~N~~	~~R~~	~~RE~~
~~20140602 PM~~	~~N~~	~~R~~	
~~20140604 AM~~	~~N~~	~~N~~	~~UD~~
~~20140605 AM~~	~~N~~	~~N~~	~~UD~~
~~20140605 PM~~	~~N~~	~~R~~	
~~20140822 AM~~	~~N~~	~~C~~	~~NE~~
~~20140822 PM~~	~~N~~	~~N~~	
~~20140827 AM~~	~~N~~	~~R~~	~~NE~~
~~20140909 PM~~	~~N~~	~~R~~	~~NE~~
~~20140910 AM~~	~~N~~	~~N~~	~~NE~~
~~20140911 AM~~	~~N~~	~~R~~	~~NE~~
~~20140915 AM~~	~~N~~	~~R~~	~~RE~~
~~20140915 PM~~	~~N~~	~~R~~	
~~20150527 PM~~	~~N~~	~~R~~	~~NE~~
~~20150528 AM~~	~~N~~	~~R~~	~~UD~~
~~20150528 PM~~	~~N~~	~~R~~	
~~20150604 PM~~	~~N~~	~~C~~	~~RE~~
~~20150604 AM~~	~~N~~	~~N~~	

~~20150605 PM~~	~~N~~	~~C~~	~~RE~~
~~20150605 AM~~	~~N~~	~~R~~	
~~20150608 PM~~	~~N~~	~~R~~	~~UD~~
~~20150608 AM~~	~~N~~	~~R~~	
~~20150609 PM~~	~~N~~	~~R~~	~~UD~~
~~20150609 AM~~	~~N~~	~~R~~	
~~20150610 PM~~	~~N~~	~~R~~	~~UD~~
~~20150610 AM~~	~~N~~	~~R~~	
~~20150813 AM~~	~~N~~	~~R~~	~~RE~~
~~20150813 PM~~	~~N~~	~~R~~	
~~20150814 AM~~	~~N~~	~~R~~	~~UD~~
~~20150814 PM~~	~~N~~	~~R~~	
~~20150817 AM~~	~~N~~	~~R~~	~~UD~~
~~20150817 PM~~	~~I~~	~~R~~	
~~20150818 AM~~	~~N~~	~~N~~	~~UD~~
~~20150818 PM~~	~~N~~	~~N~~	
~~20150819 AM~~	~~N~~	~~N~~	~~UD~~
~~20150820 AM~~	~~N~~	~~R~~	~~UD~~
~~20150821 AM~~	~~I/II~~	~~R~~	~~UD~~
~~20150821 PM~~	~~N~~	~~R~~	
~~20150824 AM~~	~~N~~	~~N~~	~~UD~~
~~20150824 PM~~	~~N~~	~~R~~	
~~20150825 AM~~	~~N~~	~~R~~	~~NE~~
~~20150825 PM~~	~~N~~	~~R~~	

~~*On May 14, 2013 a roll-induced NPF event was observed from the field station after the flight.~~

695

Table 3: Summary of the ground-based roll-induced NPF observations. BT = begin time of roll-induced NPF observation, ET = end time of roll-induced NPF observation, D_p = geometric mean particle diameter of roll-induced NPF event, Coverage = the time that subsequent roll-induced NPF events spent on top of the measurement station divided the total time it took for the subsequent roll-induced NPF events to move over the measurement site.

Date	BT [hours]	ET [hours]	D_p [nm]	GR [nm/h]	Coverage
20060921	11:50	12:57	13		
20070416	12:30 16:49 19:49	15:11 18:25 21:10	7 15 20	1.9	0.65
20070610	15:10 19.21	15:50 20:00	12 30	4.3	0.27
20090510	13:59	15:23	12		
20100312	10:57	11:46	4		
20100418	15:10	16:14	9		
20100419	10:36	11:55	7		
20110602	12:15 16:58	13:29 17:55	15 21	1.3	0.39
20110912	11:29	12:54	7		
20110930	16:47	18:20	9		
20120328	10:24 13:57 17:05	11:03 14:55 18:04	4 10 12	1.2	0.34
20120331	12:28	14:24	7		
20120405	11:08 14:29	12:02 15:53	9 12	1.0	0.48
20120409	10:42	13:13	7		
20120430	13:09 15:37	14:47 16:56	9 15	2.6	0.78
20130308	15:41	16:24	6		
20130328	12:04 16:03	13:03 17:35	6 10	0.8	0.46
20130508*	09:36	10:09	4	1.8	
20130511	13:03 16:12	14:23 18:00	12 19	1.8	0.64
20130514	13:53	15:07	13		

20130523	08:13 10:29 16:55 20:00	8:57 11:00 17:26 20:34	9 12 18 20	2.1	0.19
20140327	13:40 16:27	15:21 18.28	5 15	3.6	0.77
20140402	09:34 12:21	10:36 13:17	5 8	2.0	0.53
20150821	09:44	11:57	10		
20150913	09:59 14:48	10:59 16:43	8 18	1.9	0.43
20160415	13:07	15:15	6		
20170324	15:15	17:39	7		
20170424	13:39 17:15	14:44 18:05	4 11	2.0	0.43
20170604	11:23	12:50	7		

*For May 8, 2013 the GR was determined from the zeppelin data when the zeppelin was consecutively flying through the roll-induced NPF event (Fig. E5).